universität wien

MASTERARBEIT | MASTER'S THESIS

Titel | Title

Comparative study of SIFamide-like immunoreactive neurons in the eucheliceratе central nervous system

verfasst von | submitted by

Ines Müller BSc

angestrebter akademischer Grad | in partial fulfilment of the requirements for the degree of

Master of Science (MSc)

Wien | Vienna, 2025

Studienkennzahl lt. Studienblatt	Degree programme code as it appears on the student record sheet:	UA 066 831
Studienrichtung lt. Studienblatt	Degree programme as it appears on the student record sheet:	Masterstudium Zoologie
Betreut von	Supervisor:	Dr. Georg Brenneis

Acknowledgements

Firstly, I am extremely thankful for all the people who provided these fascinating and wonderful animals, making this project possible.

I also could not have undertaken this journey without my supervisor Dr. Georg Brenneis, who shares my passion for chelicerates and supported me throughout this thesis not only with his vast knowledge but also his humour.

I would like to extend my sincere thanks to the heads of the Department of Evolutionary Biology (University of Vienna) Univ.-Prof. DDr. Andreas Wanninger and Univ.-Prof. Mag. Dr. Mihaela Pavličev that I was able to use the facilities and resources needed to achieve my thesis. I am also thankful for the members and entire staff of the department for their help and their good company.

I had the pleasure of working with aspiring master's students and friends and want to thank Paul Arthur Höller BSc MSc, Maximillien Jadin BSc and Abby Šetena BSc, in particular for their emotional support and always being my shoulders to lean on.

Additionally, I am grateful for all the love and support from my mother Beatrix Müller, my aunt Astrid Vogelsinger, my grandmother Elisabeth Vogelsinger, my brother Jonas Müller, my father Michael Müller, my partner Marcel Pritz and my geckos Mochi, Taco and Schupfnudel.

Abstract

The evolutionary history of the Chelicerata (spiders, scorpions, ticks, mites and kin) is heavily debated due to considerable incongruities between phylogenetic hypotheses based on (mostly external) morphological characters and those generated from molecular datasets. In the past decades, comparative studies taking a closer look at the arthropod central nervous system (CNS) and its associated structures have produced comprehensive neuroanatomical datasets that can be analysed against the background of competing phylogenetic hypotheses.

In this context, one promising avenue is the study of the spatial expression of neuroactive substances (e.g. neuropeptides), in particular those that enable to reliably identify individual neurons for cross-taxa comparison. SIFamide is a highly conserved neuropeptide in arthropods, and first data for ticks and pycnogonids (sea spiders) indicate that characteristic SIFamide-immunoreactive neuron patterns are present in the chelicerate CNS.

Extending these preliminary findings, this study employed fluorescent immunolabeling coupled with confocal laser scan microscopy to describe and compare the SIFamide-immunoreactive neurons in the CNS of five additional chelicerate groups. Among taxon-specific patterns, several neuron types can be identified that display very similar soma positions and projections across taxa and are therefore proposed to be homologous. Given their presence in most of the groups studied, however, these neurons do not contribute to the current debate about euchelicerate relationships. On the other hand, one chelicerate brain neuron type with soma in the anterior protocerebrum and contralaterally descending main neurite shows striking similarities to SIFamide-immunoreactive neurons in all insects studied so far and potentially also in crustaceans. This indicates their homology across arthropod subphyla and thus potentially reveals a shared feature that dates back to the last common ancestor of arthropods.

Zusammenfassung

Die Evolutionsgeschichte der Chelicerata (Spinnen, Skorpione, Zecken, Milben und Verwandte) ist aufgrund erheblicher Unstimmigkeiten zwischen phylogenetischen Hypothesen, die auf (meist äußeren) morphologischen Merkmalen basieren, und solchen, die aus molekularen Datensätzen generiert wurden, stark umstritten. In den letzten Jahrzehnten haben vergleichende Studien, die sich eingehender mit dem Zentralnervensystem (ZNS) von Arthropoden und den damit verbundenen Strukturen befassen, umfassende neuroanatomische Datensätze hervorgebracht, die vor dem Hintergrund konkurrierender phylogenetischer Hypothesen analysiert werden können.

In diesem Zusammenhang ist die Untersuchung der räumlichen Expression neuroaktiver Substanzen (z. B. Neuropeptide) vielversprechend, insbesondere solcher, die eine zuverlässige Identifizierung einzelner Neuronen für Taxonomie-übergreifende Vergleiche ermöglichen. SIFamid ist ein hochkonserviertes Neuropeptid in Arthropoden, und erste Daten für Zecken und Pycnogoniden (Asselspinnen) deuten darauf hin, dass charakteristische SIFamid-immunreaktive Neuronenmuster im ZNS der Cheliceraten vorhanden sind.

Zusätzlich zu diesen vorläufigen Ergebnissen wurden in dieser Studie fluoreszierende Immunmarkierungen in Verbindung mit konfokaler Laserscanning-Mikroskopie eingesetzt, um die SIFamid-immunreaktiven Neuronen im ZNS von fünf weiteren Cheliceraten-Gruppen zu beschreiben und zu vergleichen. Unter den taxonspezifischen Mustern lassen sich mehrere Neuronentypen identifizieren, die über Taxa hinweg sehr ähnliche Soma-Positionen und Projektionen aufweisen und daher als homolog angesehen werden. Angesichts ihres Vorkommens in den meisten der untersuchten Gruppen tragen diese Neuronen jedoch nicht zur aktuellen Debatte über die Beziehungen zwischen Eucheliceraten bei. Andererseits weist ein Cheliceraten-Hirnneuronentyp mit Soma im vorderen Protocerebrum und kontralateral absteigender Hauptneurit auffällige Ähnlichkeiten mit SIFamid-immunreaktiven Neuronen in allen bisher untersuchten Insekten und möglicherweise auch in Krebstieren auf. Dies deutet auf ihre Homologie über die Subphyla der Arthropoden

hinweg hin und offenbart somit möglicherweise ein gemeinsames Merkmal, das bis zum letzten gemeinsamen Vorfahren der Arthropoden zurückreicht.

Table of Contents

Introduction

Chelicerates and their contested phylogeny

Chelicerates are a subphylum of arthropods, including spiders, scorpions, ticks and kin, which emerged in the early Paleozoic. They are a morphologically diverse animal group (Howard et al., 2020) and with over 120,000 extant species described across 14 orders, they are also one of the most species-rich metazoan lineages (Sharma & Gavish, 2024). However, their phylogeny is still highly discussed and far from completely understood.

In the last two decades, molecular studies have confirmed the traditional view that pycnogonids, sea spiders, are the sister group to all other extant chelicerates that form the Euchelicerata (Ballesteros & Sharma, 2019; Ballesteros et al., 2019; Lozano-Fernández et al., 2019; Nolan et al., 2020; Sharma & Gavish, 2024). By contrast, within Euchelicerata neither morphological nor genetic analyses have so far provided stable phylogenetic hypotheses (Gainett et al., 2024; Howard et al., 2020; Nolan et al., 2020). One of the most controversial issues is the placement of the marine horseshoe crabs (Xiphosura) and the question of whether terrestrialization in chelicerates took place only once or several times independently (Garwood & Dunlop, 2024; Howard et al., 2020; Lozano-Fernández et al., 2019). The traditional view derives from morphological studies focusing --among others-- on the respiratory organs, and places xiphosurans as the sister group to all terrestrial chelicerates, the Arachnida (e.g. Ballesteros & Sharma, 2019; Nolan et al., 2020). This would mean that arachnids are monophyletic and terrestrialization likely took place only once in the chelicerate lineage (Ballesteros & Sharma, 2019; Howard et al., 2020; Shultz, 2007). By contrast, most recent studies conducted using genetic datasets conclude that xiphosurans are nested within the terrestrial taxa, making arachnids not only paraphyletic but also the occurrence of multiple terrestrialization events plausible (Ballesteros & Sharma, 2019; Ballesteros et al., 2022; Lozano-Fernández et a., 2019; Nolan et al., 2020). At the same time, however, these genetic analyses fail to conclusively resolve the exact position of xiphosurans.

Beyond this unstable position of horseshoe crabs, also the relationships of many arachnid taxa are still a matter of debate. For instance, Solifugae (sun spiders, camel spiders) were proposed to be the sister group to Pseudoscorpiones (book scorpions), forming the group Haplocnemata, due to eight putative synapomorphies (Gainett et al., 2024). These synapomorphies are based primarily on external morphological characters, like their chelicerae and leg structure (Gainett et al., 2024; Shultz, 2007). However, in post-hoc evaluations, questions arose pertaining to their validity (Gainett et al., 2024; Shultz, 2007) since some of these "synapomorphies" can be found also in other chelicerate taxa and only three out of the eight proposed synapomorphic characters are unique to Haplocnemata (Gainett et al., 2024).

In molecular studies, Haplocnemata are not supported and solifuges are variably recovered in close proximity to Ricinulei (hooded tick-spiders), Palpigradi (microwhip scorpions) or Acariformes (acariform mites). Beyond this, the clade of solifuges and pseudoscorpions was refuted, based on the lack of systemic homeobox gene duplications, as is characteristic for pseudoscorpions and pulmonate arachnids which seem to share an ancient whole genome duplication (Gainett et al., 2024). Mirroring the xiphosuran case, however, the exact placement of solifuges in the phylogenetic tree is unsolved (Gainett et al., 2024). Comparable uncertainties persist for various other euchelicerate groups.

These persisting incongruities between phylogenetic hypotheses showcase that reliance on molecular and (predominantly) external morphology-based datasets alone may not suffice to resolve chelicerate evolution. This calls for careful comparative investigation of additional data sources, such as internal morphology, microanatomy, or development to expand the data basis for phylogenetic analyses. In this regard, the study of chelicerate neuroanatomy has the potential to provide useful information.

General morphology of the chelicerate central nervous system (CNS)

As in all arthropods, the CNS of chelicerates is formed by segmentally repeated units, the neuromeres. In most chelicerates, these neuromeres fuse during development into a compact "synganglion", accompanied by a posterodorsal bending of the anterior neuraxis,

leading to a characteristic dorsal flexure of the three anterior brain neuromeres (proto-, deuto- and tritocerebrum) (Babu, 1985; Lehmann et al., 2016; Loesel et al., 2013; Smarandache-Wellmann, 2016). This process renders the originally anterior protocerebrum the most dorsal unit of the adult brain (e.g. Doeffinger et al., 2010; Smarandache-Wellmann, 2016; Sombke et al., 2019). The protocerebrum contains major integration centers, for example the arcuate body and the mushroom bodies (e.g. Babu, 1985; Lehmann et al., 2016). The arcuate body is a crescent-shaped neuropil located posterodorsally in the protocerebrum (e. g. Lehmann et al., 2016; Richter et al., 2016) and can generally be distinguished into two or more layers (see Sombke et al., 2019; Stemme & Pfeffer, 2021). Anterior to the arcuate body, there are the mushroom bodies. The appearance of the mushroom bodies is quite diverse throughout chelicerates (Babu, 1985). In amblypygids and xiphosurans, the mushroom bodies constitute a big portion of the protocerebrum (Babu, 1985; Sinakevitch et al., 2020). However, for example in pseudoscorpions the mushroom bodies are hardly identifiable (Stemme & Pfeffer, 2021). The deutocerebrum is associated with the cheliceral neuropil and the tritocerebrum with the pedipalpal neuropil (Loesel et al., 2013). The ventral nervous system (VNS) is composed of the walking leg and the opisthosomal neuropils (Lehmann et al., 2016).

Evolutionary conserved neuron types in the arthropod central nervous system

Comparative studies of the arthropod CNS and its development have a long tradition (e.g. Babu, 1985; Hanström, 1928; Loesel et al., 2013). Beyond novel insights into nervous system architecture and general evolutionary trends, several recent studies have produced datasets that can be analysed against the background of competing phylogenetic hypotheses (e.g. Harzsch et al., 2005; Kutsch & Breidbach, 1994; Ungerer & Scholtz, 2008). For instance, immunolabeling of serotonin (5-hydroxytryptamine, 5-HT), a bilaterian-wide conserved biogenic amine serving various functions, has led to the discovery of 5-HT-immunoreactive neurons in the ventral nerve cord of diverse arthropod taxa (Brenneis & Scholtz, 2015; Harzsch, 2004; Harzsch & Waloszek, 2000; Sombke & Stemme, 2017; Stemme et al., 2017; Wolf & Harzsch, 2012). Based on the positions of their somata and characteristic axonal and dendritic projections, part of these neurons are individually identifiable (see Kutsch &

Breidbach, 1994, for concept of individually identifiable neurons), which enables their direct comparison and homologization across taxa and evaluation in phylogenetic contexts.

In similar fashion, a comparative study of the CNS in more than 40 pycnogonid taxa, revealed conserved patterns of individual identifiable neurons and neuron groups immunoreactive for the neuropeptide SIFamide (Brenneis et al., in prep). While some of these neurons are located in the brain, others are found in the segmental ganglia of the VNS, where they occur in two mutually exclusive patterns across the pycnogonid families (Brenneis et al., in prep). Mapping these segmental patterns on existing phylogenetic hypotheses, it was discovered that their distribution aligns with modern molecular pycnogonid phylogenies (e.g., Ballesteros et al., 2021) and contradicts long-held evolutionary scenarios based on external morphology (e.g., Munilla, 1999; Stock, 1994).

The arthropod neuropeptide SIFamide

SIFamides are a family of neuropeptides found in arthropods and are highly conserved throughout this phylum. In all arthropods studied so far, only a single SIFamide form is present, consisting of 11-12 amino acid residues with the characteristic SIF-motif at the C-terminus (Gellerer et al., 2015).

Apart from the pycnogonid CNS, characteristic patterns of SIFamidergic neurons have also been observed in various insect groups, for example the grey flesh fly *Neobellieria bullata*, the honeybee *Apis mellifera* and the desert locust *Schistocerca gregaria* (Arendt et al., 2015). They all share two pairs of individually identifiable neurons with somata in the anteromedian brain (pars intercerebralis). Their neurites innervate the brain and project posteroventrally into the ventral nerve cord (Gellerer et al., 2015). Furthermore, SIFamide-immunoreactive neurons and their projections have also been recorded in crustaceans, including the amphipod *Parhyale hawaiensis* and the marbled crayfish (Polanska et al., 2007; Raspe et al., 2023). In *P. hawaiensis*, for instance, Raspe et al. (2023) found three individually identifiable neuron somata in the central brain.

These examples demonstrate the feasibility of describing SIFamidergic neuronal patterns down to the level of individual cells in different arthropod groups with the potential to be phylogenetically informative.

Thesis aims: Description and comparison of SIFamidergic neuronal patterns in selected euchelicerate taxa and evaluation of potential phylogenetic information content

In contrast to pycnogonids, virtually nothing is known about SIFamide-immunoreactive neurons in the euchelicerate CNS. While several analyses have confirmed the general presence of SIFamide in several euchelicerate taxa through transcriptomics (Christie et al., 2011; Christie & Chi, 2015; Simo et al., 2013), only a single study cursorily describes SIFamide-immunoreactive neurons and their projections in a tick, suggesting the presence of characteristic neuron types (Šimo et al., 2009; Šimo et al., 2013).

In this study, the aim is to firstly describe SIFamide-immunoreactive neurons and their patterns in selected euchelicerate taxa. In addition to evaluating them in the context of euchelicerate phylogeny, they will be compared to other arthropod groups, to explore the potential of homologizing SIFamidergic neurons with their specific projection patterns across Arthropoda and reconstruct ancestral characteristics of SIFamidergic components in the arthropod CNS.

Material and Methods

Animals investigated in this study

The CNS of five orders of chelicerates was investigated: Araneae (spiders), Amblypygi (whip spiders), Scorpiones (scorpions), Pseudoscorpiones (book scorpions) and Solifugae (sun spiders). In addition, the CNS of Xiphosura (horseshoe crabs) was superficially investigated.

Adult females and juveniles of *Cupiennius salei* (spider) were provided by Benjamin Steiner MSc (Division Neurobiology, University of Vienna, Austria) and already fixed prior to this study (details Table 1). Individuals of two species of the genus *Phrynus* (whip spider), *Phrynus maesi* and *Phrynus barbadensis* and one individual of *Paraphrynus* sp. were provided by Dr. Michael Seiter (formerly University of Vienna, Austria) and kept in-house in tall glass containers with earthy substrates and pieces of bork and cared for until fixation (details Table 1). Adult females of *Euscorpius italicus* (scorpion) were also kept in our husbandry in square plastique containers (details Table 1). They were supplied by Dr. Torben Stemme (formerly University of Ulm, Germany), who also collected adult individuals of *Chelifer cancroides* (pseudoscorpion, both sexes; (details Table 1). Juvenile specimens of *Rhagodes* sp. (sun spider) were given to us by Clemens Schweiger BSc (details Table 1). Juvenile *Limulus polyphemus* (horseshoe crab) were provided by Dr. Carsten Wolff (Marine Biological Laboratory, Woods Hole, USA).

Table 1: Species, ontogenetic stages, specimen numbers and methods used in this study.

Taxon	Species	Life stage	Numbers	Methods – Vibratome sections
Araneae	- *Cupiennius salei*	- Adult - Juvenile	- 4 - 2	- Horizontal – 150 µm - Horizontal – 100 µm and wholemount
Amblypygi	- *Phrynus maesi* - *Phrynus barbadensis* - *Paraphrynus* sp.	- Adult - Adult - Adult	- 2 - 1 - 1	- Horizontal – 100-150 µm - Horizontal – 150 µm - Cross sections – 120 µm
Scorpiones	- *Euscorpius italicus* - *Euscorpius* sp.	- Adult - Juvenile	- 4 - 1	- Horizontal – 150 µm; cross sections – 130 µm - Horizontal – 70 µm

Pseudoscorpiones	-	*Chelifer cancroides*	-	Adult	-	5	- Horizontal – 200 µm - Cross sections – 130 µm - Sagittal sections – 150 µm
Solifugae	-	*Rhagodes* sp.	-	Juvenile	-	2	Horizontal – 120 µm

To fix the CNS of the spiders and amblypygids, each animal was first sedated with CO_2 in the laboratories of the Division of Neurobiology at the University of Vienna, followed by quick removal of all extremities and the opisthosoma with micro-scissors. The prosoma was briefly placed into 70% ethanol to reduce trapping of air bubbles between cuticle and external hairs before being transferred into 4% paraformaldehyde (PFA; Sigma-Aldrich; Cat.no. 158127) in 0.1M phosphate-buffered saline (PBS) at ambient temperature. Within the next hour, it was then taken out and the dorsal peltidium opened up in 0.1M PBS to improve tissue penetration of the fixative. Afterwards, it was again put into 4% PFA and stored overnight at 4°C. In case of longer storage prior to further use, the "opened" prosoma was placed into cryobuffer (0.05 M sodium phosphate buffer, 300 g/L sucrose, 30% (v/v) ethylene glycol, 10 g/L polyvinylpyrrolidone) and stored in a freezer at -20 °C.

Fixation of scorpions, pseudoscorpions and solifuges was preceded by placing the animals briefly inside the freezer for sedation, larger specimens (like the scorpions) up to ten, the smaller ones for one to three minutes. From this point onwards, the processing was identical to that of the spiders and amblypygids. For the final dissection the PFA-solution was replaced with 0.1M PBS.

Vibratome sectioning

Apart from the pseudoscorpions, the CNS of all species investigated was fully dissected in 0.1M PBS. Due to the small body size of the pseudoscorpions and difficulties of obtaining intact dissections due to the extensive tracheal system spanning through their CNS, the whole prosoma was used for the subsequent procedures. Each CNS/prosoma was then coated in Poly-L-Lysin (0.1 mg/ml; Sigma-Aldrich, Cat.no. P4707) to improve attachment of the tissue/cuticle to the 5% low-gelling agarose (w/v; Sigma-Aldrich, Cat.no. A9414) that was

used as embedding medium. Prior to embedding, the agarose powder was mixed with distilled water and heated just under 100°C until the agarose was dissolved. The specimens were oriented under a stereomicroscope until hardening of the agarose at room temperature (RT). They were then put into the refrigerator (4°C) and when not processed immediately, stored there overnight. Samples were subsequently trimmed into blocks. These blocks were cut into horizontal, cross sections and in the case of the pseudoscorpion, also in sagittal sections using a Leica VT 1200 vibratome. The thickness of the sections depended on the size of the respective CNS and ranged from 70µm up to 200µm (Table 1).

Fluorescent immunohistochemistry and nuclear staining

To permeabilize the tissues for better antibody penetration, the sections were washed two times for at least 15 minutes in PBTx (0.1M PBS containing 0.5% Triton X-100 and 1.5% dimethylsulfoxide [DSMO]) before putting them in a 6% normal goat serum blocking solution (NGS; Invitrogen, PCN5000; in PBTx) on a rocking platform for one hour. After incubation, the sections were washed several times in PBTx over the course of two hours before incubation with the secondary antisera again overnight at RT. This solution included additionally the DNA marker DAPI (4´,6-diamidino-2-phenylindole; see Table 2) to visualize cell nuclei. Subsequent to incubation, the sections were washed several times in PBTx before rinsing them in 0.1M PBS. They were then sorted into well plates according to their chronological order.

The sections were mounted on microscopic slides in Vectashield® Mounting Medium (Vector Laboratories, Inc; Cat.no. H-1000) for sections thinner than 150 µm and in Mowiol® 4-88 + DABCO (Sigma-Aldrich [Roth], Cat.no. 0713 + 0718) for sections of 150 µm or above. In the case of two individuals of *Chelifer cancroides* the sections were mounted in RapiClear® (SunJin Lab, Cat.no. RC149001; thickness of sections: 200 µm).

Table 2: Primary and secondary antibodies used in this study.

Labeling reagent	Dilutions, specifications
Primary	
Monoclonal mouse anti-synapsin (RRID AB_528479)	1:1000, Developmental Studies Hybridoma Bank, clone 3C11

Polyclonal rabbit anti-SIFamide	1:2000; Suntori Institute for Bioorganic Research, Osaka, Japan, Dr. A. Yasuda
Secondary	
Polyclonal goat anti-mouse IgG (H+L) cross-adsorbed secondary antibody, Alexa Fluor™ 568 (RRID AB_2534072)	1:500 or 1:750; Invitrogen, Cat.no. A11004
Polyclonal goat anti-rabbit IgG (H+L) cross-adsorbed secondary antibody, Alexa Fluor™ 488 (RRID AB_143165)	1:500 or 1:750; Invitrogen, Cat.no. A11008
DAPI	1:1000; Sigma-Aldrich, Cat.no. D9542

Antibody characterization

The SIFamide antiserum used in this study was raised in rabbit against a crustacean-SIFamide (injected antigen: Cys-GYRKPPFNGSIF-$CONH^2$ conjugated to bovine serum albumin). This neuroactive peptide was extracted and characterized in the crayfish *Procambarus clarkii* through topological mass spectrometry by Dr. A. Yasuda and colleagues (2004). Their analysis revealed an amino-acid sequence of Gly–Tyr–Arg–Lys–Pro–Pro–Phe–Asn–Gly–Ser–Ile–Phe (Yasuda et al., 2004). With the help of database research, a very similar peptide to GYRKPPFNGSIFamide has been found in *Drosophila melanogaster* (Yasuda et al., 2004). This peptide differs from the crayfish GYRKPPFNGSIFamide only in the first amino acid at the N-terminus, which is Alanine instead of Glycine, strongly suggesting their homology (Yasuda et al., 2004). In addition to *D. melanogaster*, the AYRKPPFNGSIFamide peptide has been identified in several other arthropod taxa, for example in the honeybee *Apis mellifera,* the moth *Galleria mellonella* and also the tick *Ixodes scapularis*, an arachnid (e.g. Arendt et al, 2015; Gellerer et al., 2014; Verleyen et al., 2009). Nevertheless, GYRKPPFNGSIFamide and AYRKPPFNGSIFamide are not the only two forms of SIFamide. Throughout many neuropeptide studies, it was revealed that there are at least eight other forms of SIFamide, most of them differ in only one or two amino acids (e.g. Gellerer et al., 2015; Verleyen et al., 2009). Furthermore, no evidence of more than one form of SIFamide existing in one species has been found.

This high degree of sequence conservation across different arthropod subphyla and the discovery of GYRKPPFNGSIFamide in the mosquito *Anopheles gambiae* (Arendt et al., 2015;

Riehle et al., 2002), which demonstrated the Glycin-form of SIFamide also outside of crustaceans, makes SIFamide a promising candidate for comparative immunohistochemical studies. In support of this, previous studies have demonstrated strong cross-reactivity of the “crustacean”-SIFamide antiserum in additional crustacean taxa (Polanska et al., 2007; Raspe et al., 2023) and even in sea spiders (Brenneis personal communication).

In spite of the strong indications for correct target-binding of the antiserum across distantly related arthropod taxa, immunolabeled structures will be cautiously designated as SIFamide-like immunoreactive (SIFa-lir) throughout this study.

For visualization of neuropil regions, a monoclonal mouse antibody against *Drosophila* synapsin was used (“SYNORF1”; Table 1). This antibody was raised against *Drosophila* Glutathione S-Transferase (GST)-synapsin fusion protein (e.g. Drozd et al., 2020; Fabian-Fine et al., 1999; Maurer et al., 2019). The antibody binds to a highly conserved epitope and has been demonstrated to reliably mark neuropilar domains across different arthropod taxa, including chelicerates (Sinakevitch et al., 2020; Steinhoff et al., 2017, 2020, 2023; Stemme & Pfeffer, 2021; Brenneis, 2022; Frankowski et al., 2022).

Data documentation, analysis and visualization

All sections were investigated under a Nikon SMZ25 epifluorescence stereomicroscope. Brightfield and fluorescence channel z-stacks were created and merged into images with extended field of depth using the NIS-Elements software (version 5.02.03).

In a second step, the sections were scanned with a Leica DM6000 confocal laser scanning microscope (CLSM) paired with a Leica TCS SP5 scan unit. The laser lines used were a 405 Diode laser for DAPI signal, a DPSS 561 laser for synapsin signal and an Argon laser (wavelength of 488 nm) for SIFamide signal. Depending on the size of the nervous system, the glycerol immersion objectives used ranged from 10x to 63x, the latter primarily applied for details. The resulting z-stacks were processed, analysed and documented through snapshots with the 3D reconstruction software program “Imaris” (version 7.6.5; Oxford

Instruments) and the illustrations were done using Adobe Illustrator (version 25.3.1; Adobe Inc.).

Nomenclature and descriptions

The terminology used in this study is based on Babu (1985), Loesel et al. (2013), Lehmann et al. (2016) and Richter et al. (2010).

All horizontal images of the CNSs are positioned with anterior directed to the top (unless stated otherwise) whereas cross sections are oriented with dorsal to the top. Descriptions regarding positions are given in relation to the body axis, which does not necessarily align with the neuraxis. Major structures in the protocerebrum like the arcuate body and mushroom bodies will act as landmarks when describing SIFa-lir neurons and their projections.

Results

Across all taxa studied, the identified SIFa-lir neurons are of the unipolar type. The somata of most of them are located in the protocerebrum. Notably, single SIFa-lir somata, small SIFa-lir clusters of somata and their nuclei are much bigger compared to the cells surrounding them (e.g. globuli cells).

SIFa-lir signal is also found in the major neuropilar regions of the protocerebrum: throughout the layers of the arcuate body and parts of the mushroom bodies, specifically in the amblypygids. In none of the taxa studied, however, the neuronal somata contributing to the SIFa-lir domains within these integration centers could be identified.

Amblypygi: *Phrynus maesi*, *Ph. barbadensis* and *Paraphrynus* sp.

Consistently labelled SIFa-lir neurons in the CNS

In the protocerebrum four dorsal somata were identified in each hemisphere (Figs. 1A, 2A, 2A', 3A, 4). Three somata cluster together whereas the fourth soma can be found aside and medial to this cluster (Figs. 1A, 2A, 2A', 3A, 4). All somata are located ventral to the big mushroom body lobes and anterodorsal to the arcuate body (Figs. 1A, 2A, 2A', 4). In addition to these four somata, there is a dorsolateral cluster located in the soma cortex lateral to the

protocerebral neuropil, situated on the same level as the arcuate body (Figs. 1B, 1C, 2B', 3D, 4).

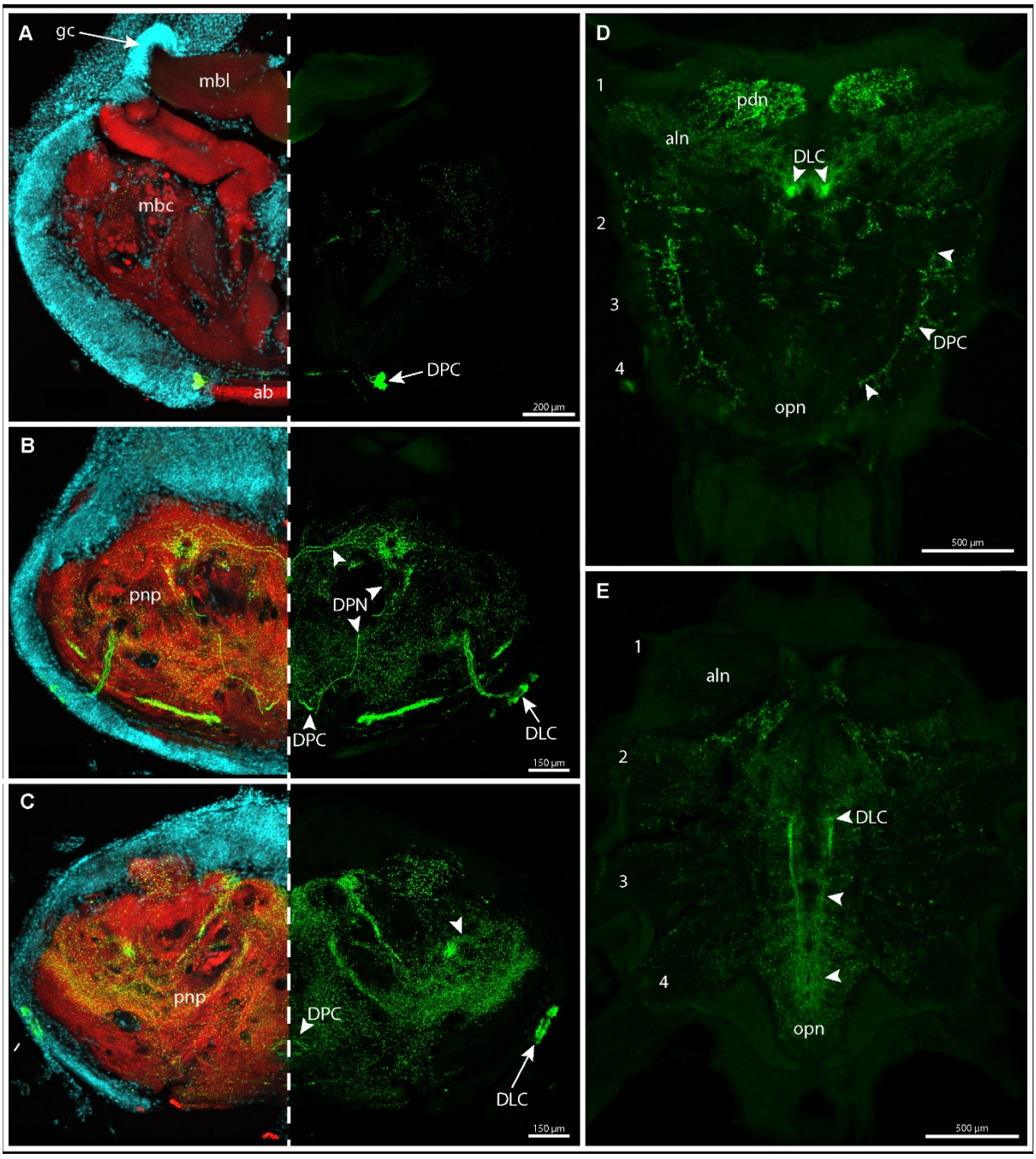

Figure 1: Overview of the SIFa-lir structures in the CNS of *Phrynus maesi*. Maximum intensity projections of CLSM scans (A-C) or stereomicroscopic image stacks (D & E) of horizontal vibratome sections. Arrows indicate neuronal somata, arrowheads indicate their projections. **A-C.** The left half of each image shows SIFa-lir (green) together with synapsin immunolabeled structures (red) and nuclear staining (DAPI; cyan), while the other half was mirrored to show the SIFa-lir structures separately. **D & E.** Only the SIFa-lir of the VNS is shown.

A. First protocerebral section, where the dorsoposterior neuron cluster (DPC) is visible posterior to the mushroom bodies and anterior to the arcuate body. **B.** Next protocerebral section. Arrowheads show the trajectory of the dorsoposterior neuron (DPN) from the posterior to the anterior protocerebral brain neuropil. The arrowhead close to the midline depicts the neurite bundle of the DPC projecting ventral. Note the first appearance of the dorsolateral neuron cluster (DLC) on the edge of the posterolateral protocerebral neuropil with its neurite bundle projecting into it. **C.** Next protocerebral section. Part of the DLC is still seen in the same position as before (arrow), part of its neurite bundle is visible in the medial part of the protocerebral neuropil (arrowhead). The neurites of the DPC are about to cross over in the posteromedian protocerebral neuropil. **D.** Section of the VNS. Lateral arrowheads depict the path of the DPC neurites. The two strongly SIFa-lir "dots" correspond to the neurite projection tracts of the DLCs. **E.** Section of the VNS further ventral. Arrowheads show the neurite projection tracts of the DLCs.
Abbreviations: ab = arcuate body, aln = antenniform leg neuropil, DPC = dorsoposterior neuron cluster, DPN = dorsoposterior neuron, DLC = dorsolateral neuron cluster, gc = globuli cells, mbc = mushroom body calyx, mbl = mushroom body lobes, opn = opisthosomal neuropil, pdn = pedipalpal/tritocerebral neuropil, pnp = protocerebral neuropil, 1-4 = walking leg neuropils

Dorsoposterior neuron cluster (DPC)

The neurites of these neurons form a bundle that projects ventrally through the protocerebral neuropil anterior to the arcuate body (Figs. 1A-C, 2A-B', 4). Above the oesophagus, the bundles cross contralaterally and project to the outer edge of the posterior part of the brain neuropil between the deuto- and tritocerebral brain regions (Figs. 1C, 2B, 2B', 3C, 4). Starting from this point, they run dorsally along the entire length of the VNS (Figs. 1D, 3F, 4).

Dorsoposterior neuron (DPN)

The soma of this neuron is situated close to the DPC, but slightly more medially in the posterior protocerebral neuropil (Figs. 2A, 2A', 3A, 4). Its neurite projects differently than the DPC bundle. It projects horizontally to the anterior side of the protocerebral neuropil where it turns towards the midline (Figs. 1B, 3B, 4). Here, it overlaps with its contralateral counterpart (Fig. 1B). Before crossing over into the other body half, it makes a sharp bend, which can be seen in the sections as a "v-shape" (Fig. 1B). Once in the contralateral hemisphere, it branches into a network of delicate branches that could not be traced any further.

Dorsolateral neuron cluster (DLC)

This neuron cluster comprises about 20 somata and is situated in the lateral soma cortex, next to the protocerebral neuropil (Figs. 1B, 1C, 2A-B', 3D, 4). The cluster's neurites travel as one prominent bundle ventromedially through the proto-, deuto- and tritocerebral neuropil

(Figs. 1B, 1C, 2C, 2C', 3E, 4). In the VNS, the bundle projects parallel to its contralateral counterpart, anterior to the "ventromedial neuropil" (see Sinakevitch et al., 2020 for a thorough description) to the posterior end of the VNS (Figs. 1D, 1E, 2D, 2D', 4). These tracts are interconnected through diffuse SIFa-lir commissures (Figs. 1E, 4).

Additionally, to the main neurites, many smaller neurites branch off those neurites and build up a dense SIFa-lir network in the brain (Figs. 1B, 1C, 2B', 2C', 3E).

Posterolateral neuron (PLN)

In *Phrynus barbadensis*, another SIFa-lir soma is found posterior to the DLCs and posterolateral in the protocerebral soma cortex (Fig. 3E, 4). The neurite projects into the protocerebral neuropil (Fig. 3E, 4). Before crossing into the contralateral brain hemisphere, two collaterals branch off and run ventrally, but remain in the ipsilateral neuropil lobe (Fig. 3E, 4). In the contralateral hemisphere, the neurite bends ventrally and posteriorly before turning dorsally at the posterior edge of the protocerebral neuropil (Fig. 3E, 4). Here, it crosses back into the ipsilateral side, where it arborizes into several smaller neurites innervating the brain neuropil (Fig. 3E, 4).

While the two ipsilateral collaterals run ventrally, they get thinner before they could not be traced any further. Presumably, they branch into smaller neurites themselves which transition into the speckled network of SIFa-lir signal.

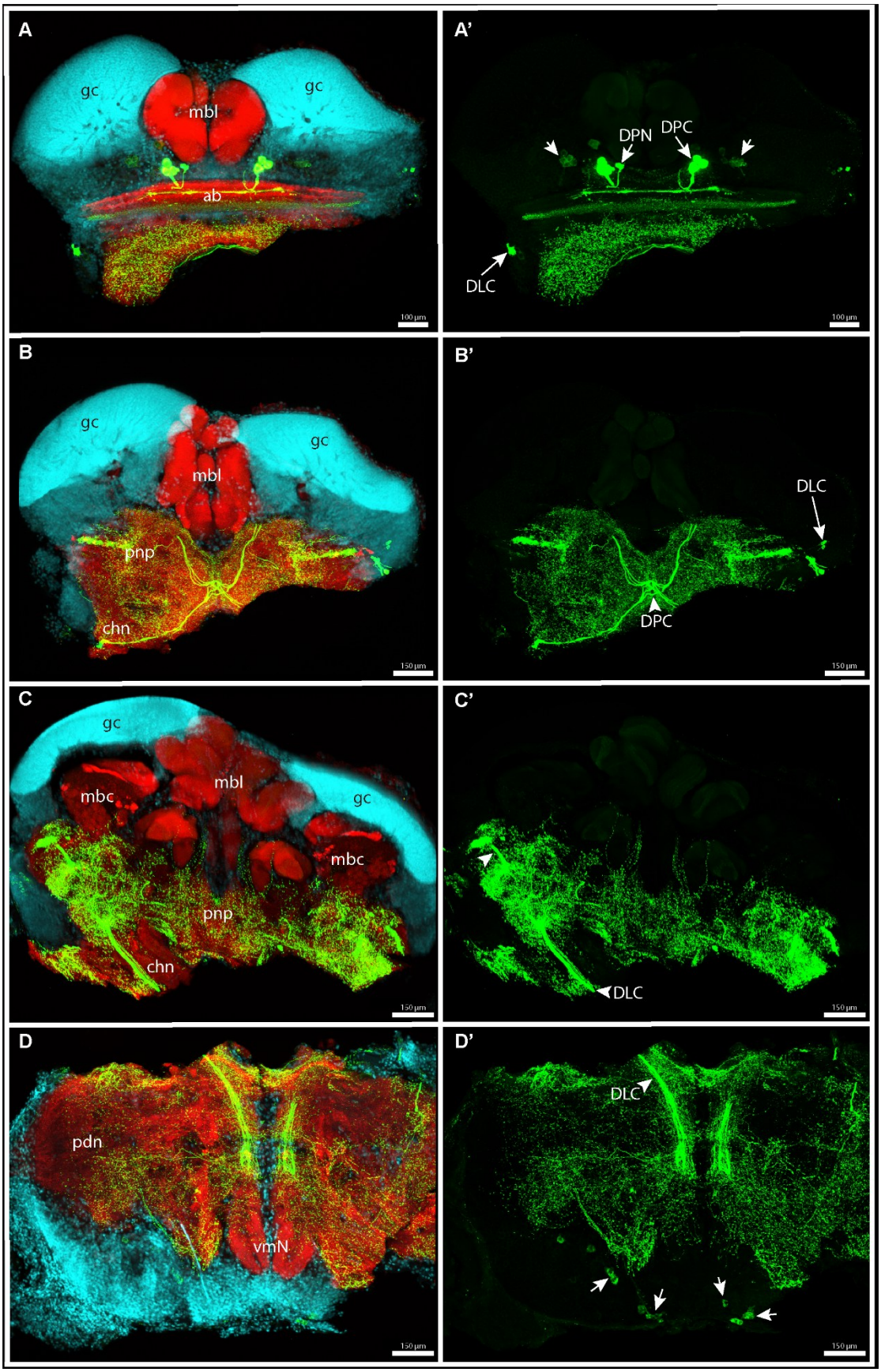
A
gc
gc
mbl
ab
100 µm
A'
DPN
DPC
DLC
100 µm
B
gc
gc
mbl
pnp
chn
150 µm
B'
DLC
DPC
150 µm
C
gc
mbl
mbc
gc
mbc
pnp
chn
150 µm
C'
DLC
150 µm
D
pdn
vmN
150 µm
D'
DLC
150 µm

Figure 2 (previous page): Overview of the SIFa-lir structures of the CNS of *Paraphrynus* sp. Maximum intensity projections of CLSM scans showing cross sections (brain and VNS were separated during dissection). Arrows indicate neuronal somata, arrowheads indicate their projections. **A-D.** SIFa-lir signal (green) against the backdrop of synapsin immunolabeled structures (red) and nuclear staining (DAPI; cyan). **A'-D'.** Only SIFa-lir signal. **A/A'.** Posterior cross section of the brain. DPN and DPC are located ventral to the mushroom body lobes and dorsal to the arcuate body. In one body half, first somata of the DLC can be seen ventrolateral to the arcuate body. Small, weakly SIFa-lir somata clusters are visible lateral to the DPCs (arrows). **B/B'.** Second most posterior brain section. The DPC neurites cross contralaterally in the protocerebral neuropil. Part of the DLC somata can be seen in the right body half. **C/C'.** One of the middle sections of the series. Arrowheads indicate the neurite projection tract of the DLC passing from the protocerebral to the deutocerebral/cheliceral neuropil. **D/D'.** Section through tritocerebrum (pedipalpal neuropil) and the VNS. The DLC neurite projection tract projects into the median part of the VNS above the ventromedian neuropil. Scattered SIFa-lir somata can be seen in the ventral soma cortex (arrows).
Abbreviations: ab = arcuate body, chn = cheliceral/deutocerebral neuropil DLC = dorsolateral neuron cluster, DPC = dorsoposterior neuron cluster, DPN = dorsoposterior neuron, gc = globuli cells, mbc = mushroom body calyx, mbl = mushroom body lobes, pdn = pedipalpal/tritocerebral neuropil, pnp = protocerebral neuropil, vmN = ventromedian neuropil

Figure 3 (next page): Details of the protocerebral neurons and their trajectories in the two *Phrynus* species. A, D & E. *Phrynus barbadensis*. **A, B, C & F.** *Phrynus maesi*. SIFa-lir signal is grey-scale inverted. Arrows indicate somata, arrowheads indicate their projections. **A.** Lateral view of the DPN and the DPCs of one protocerebral hemisphere of *Phrynus barbadensis*. In the lower left corner, two of the DPCs (*Phrynus maesi*) are shown with their nuclei (SIFamide = green, nuclei = cyan). **B.** Lateral view of the neurite from the DPN travelling anteroventrally, whereas the DPC neurites project ventrally. **C.** Detail of the crossing over of the DPC neurites to the contralateral side of the protocerebral neuropil above the oesophagus. The star (with the red outline) indicates globular extensions, boutons, of the neurites. **D.** Lateral view of the DLC and its prominent neurite bundle that extends into the protocerebral neuropil. **E.** Detail of the posterolateral neuron (PLN). Dashed line indicates the brain midline. Its neurite projects across the protocerebral neuropil to the brain midline (arrowheads), where two collaterals split ipsilateral and the "main" neurite continues contralaterally to re-emerge at the posterior edge of the protocerebral neuropil, re-enter the ipsilateral brain half and form a dense network of delicate SIFa-lir neurites. At the midline, the crossing over of the DPCs are visible. In the upper right corner, the DLC neurite bundle can be seen. **F.** Detail of the DPC neurites running along the outer edge of the walking leg neuropils in the VNS (arrowheads).
Abbreviations: DPC = dorsoposterior neuron cluster, DPN = dorsoposterior neuron, DLC = dorsolateral neuron, PLN = posterolateral neuron

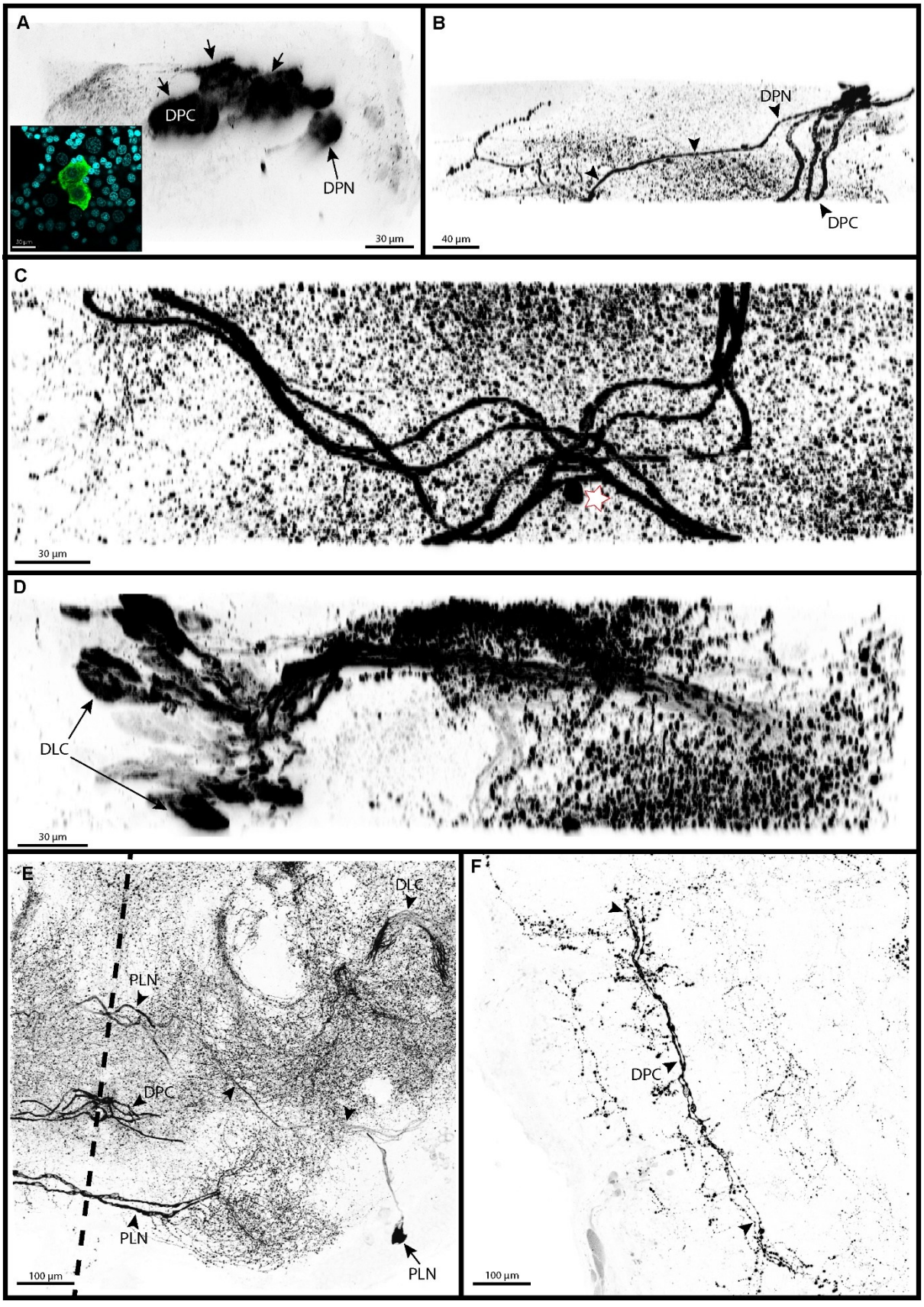
A
DPC
DPN
30 µm
B
DPN
DPC
40 µm
C
30 µm
D
DLC
30 µm
E
DLC
PLN
DPC
PLN
PLN
100 µm
F
DPC
100 µm

Weakly and/or inconsistently labelled SIFa-lir structures

SIFa-lir structures in the VNS

Apart from the neurite bundles of the DPC and the DLC, diffuse speckled SIFa-lir signal is present across the VNS of all three species studied (Figs. 1D, 1E, 2D, 2D', 3F, 4). In *Paraphrynus* sp., additional clusters of weakly stained somata could be observed within the ventral soma cortex of the VNS (Figs. 2D, 2D', 4). A shadow of a neurite from one of those clusters was seen to project into this network, potentially indicating a connection between those neurons and the SIFa-lir tracts of the VNS (Figs. 2D, 2D', 4).

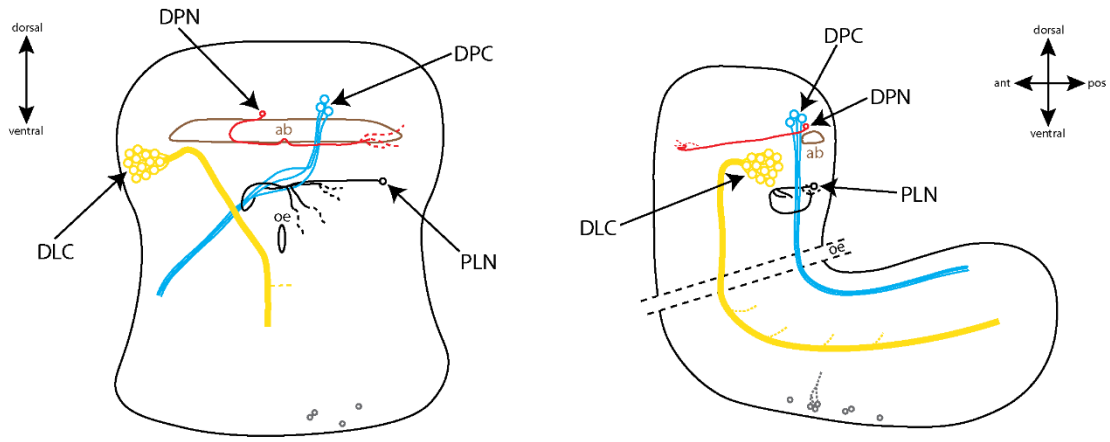

Figure 4: Schematic representations of SIFa-lir neurons and their major projections in the CNS of *Phrynus* and *Paraphrynus*. The left drawing shows an anterior view, the right shows a lateral view. Each neuron type/group is shown only for one body half (DPC – light blue; DPN – red; DLC – yellow; PLN - black). The PLN was only present in *Phrynus barbadensis*. Dashed lines indicate punctuate SIFa-lir patterns originating from neurites. Inconsistently/weakly labeled somata of the VNS are indicated in grey.
Abbreviations: ab = arcuate body, ant = anterior, DPC = dorsoposterior neuron cluster, DPN = dorsoposterior neuron, DLC = dorsolateral neuron, oe = oesophagus, PLN = posterolateral neuron, pos = posterior

Araneae: *Cupiennius salei*

Consistently labelled SIFa-lir neurons in the CNS

In each protocerebral hemisphere, six SIFa-lir somata are located between the anterior visual neuropils and the posterior arcuate body (Figs. 5A, 6A, 7).

In the lateral soma cortex near the proto- and deutocerebral boundary and ventral to the mushroom bodies, an additional somata cluster can be found (Figs. 5D, 5E, 6D, 6E). Throughout the entire brain neuropil, a high amount of varicose SIFa-lir signal is present, presumably originating from these two neuron clusters.

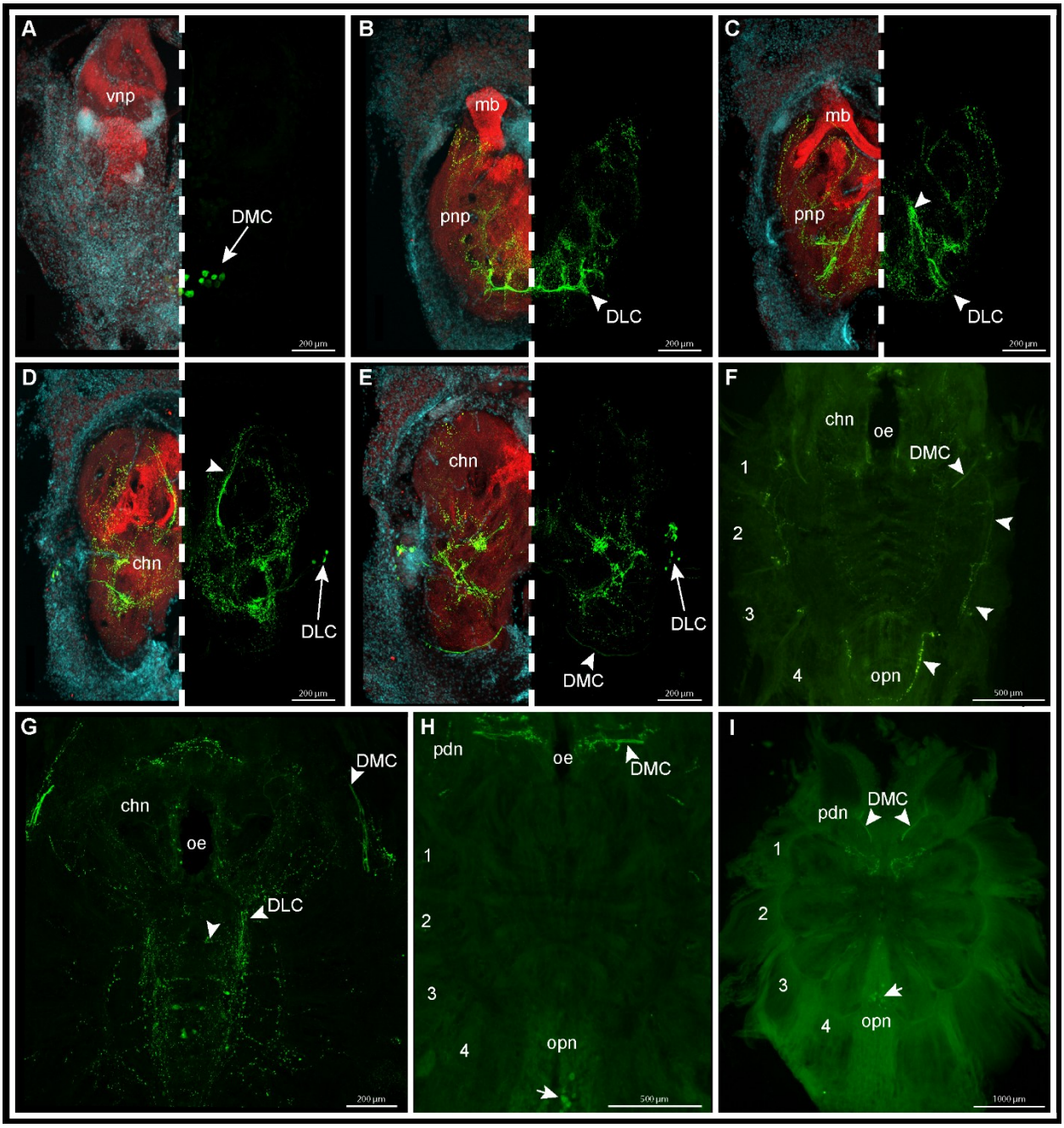

Figure 5: Overview of the SIFa-lir structures in the CNS of *Cupiennius salei*. Maximum intensity projections of CLSM scans (**A**-**E**, **G**) and stereomicroscopic image stacks (**F**, **H**, **I**) of horizontal vibratome sections. The left half of images **A**-**E** shows SIFa-lir signal (green) in the context of synapsin-immunolabeled structures (red) and nuclear staining (DAPI; cyan); the right half shows only SIFa-lir signal. Arrows indicate somata, arrowheads indicate the trajectories of their neurite projections. **A.** Dorsal protocerebral section with the dorsomedial neuron cluster (DCM) situated posterior to the visual neuropils. **B.** Second protocerebral section. The prominent transverse tract of the dorsolateral neuron cluster (DLC) is visible in the posterior protocerebral neuropil. **C.** Third protocerebral section. Posterior to the mushroom body bridge, the contralateral DLC neurite bundle splits off into the anterior part of the protocerebral neuropil (arrowhead). The remaining neurites of this bundle run ventrally. **D.** Section near the proto- and deutocerebral boundary. While the contralateral DLC

neurite bundle further innervates the brain neuropil (arrowhead), a part of the ipsilateral DLC can be seen (arrow). **E.** Deutocerebral brain section (cheliceral neuropil). In the lateral soma cortex, the remaining somata of the DLC are seen. The majority of SIFa-lir signal to their left belongs to a portion of the contralateral DLC. Along the outer edge of the posterior cheliceral neuropil, some DMC neurites are visible. **F.** Section of the cheliceral neuropil and the VNS. The DMC neurites project anterolaterally along the neuropil. One or more collaterals branch off, travel along the walking leg neuropils and surround the opisthosomal neuropil (arrowheads). **G.** Section of the anterior half of the VNS. The DMC neurites project further anteriorly. At the posterior boundary between the cheliceral neuropils, thin DLC neurites form a posteriorly projecting tract, which is connected to its contralateral counterpart by commissures (middle arrowhead). **H.** Ventral VNS section. The DCM neurites project through the tritocerebrum/pedipalpal neuropil next to the oesophagus. Weakly SIFa-lir somata are visible in the opisthosomal neuropil (arrow). **I.** Ventral-most VNS section. The DCM neurites run along the outer edge of the pedipalpal neuropil into the periphery. In the opisthosomal neuropil, there are more SIFa-lir somata (arrow).

Abbreviations: ab = arcuate body, chn = cheliceral/deutocerebral neuropil, DLC = dorsolateral neuron cluster, DMC = dorsomedial neuron cluster, mb = mushroom bodies, oe = oesophagus, opn = opisthosomal neuropil, pdn = pedipalpal/tritocerebral neuropil, pnp = protocerebral neuropil, vnp = visual neuropils, 1-4 = walking leg neuropils

Dorsomedial neuron cluster (DMC)

Depending on the individual, either all six somata or only some of them cluster more tightly together (Figs. 5A, 6A, 7), rendering distinction between neurons harder. Furthermore, the primary neurites seem to project differently to each other (Fig. 6A). Between the proto- and deutocerebral boundary the neurites disappear into the SIFa-lir meshwork in the brain, only in more ventral sections, the DMC neurites could be traced again with confidence. Presumably, some if not all neurites of the DMC form a ventrally projecting bundle, moving steadily to the midline. While a contralateral crossing of the DMC neurites above the oesophagus could not be ascertained in adult specimens, it was confirmed in the CNS wholemount of a juvenile (Fig. 6I). Next to the oesophagus, a bundle comprising at least three DMC neurites projects along the outer edge of the deutocerebral neuropil from the midline to its lateral outer edge (Figs. 5E, 5F, 6D-F, 7). One or more thin collaterals branch off this bundle and extend posteriorly into the VNS, travelling dorsally along the edge of the VNS and enclosing the opisthosomal neuropil (Figs. 5F, 6F, 6G, 7). By contrast, the main neurite bundle arches back anteromedially into the tritocerebrum/pedipalpal neuropil (Figs. 5G, 5H, 6G, 7). From this point onwards, it extends and arborizes into the pedipalpal nerve (Fig. 5I, 7).

Further complementing these DMC main bundles, another neurite projects from the midline of the deutocerebral neuropil into the VNS (Fig. 6F, 7). It extends along the inner edge of the walking leg neuropils, terminating between the border of the fourth walking leg and opisthosomal neuropil (Fig. 6F, 7).

Dorsolateral neuron cluster (DLC)

In the lateral soma cortex of the proto- and deutocerebral neuropil boundary, approximately 20 SIFa-lir somata are located slightly ventral to the mushroom bodies (Figs. 5D, 5E, 6D, 6E, 7). These somata are arranged in an anterior and a posterior subcluster with a neurite bundle emanating from each of them. (Figs. 5E, 6E, 7). After entering the proto-/deutocerebral neuropil, however, the two bundles join and project together dorsally (Figs. 5C-E, 6D, 6E, 7). Directly underneath the arcuate body, the bundle forms a prominent transverse tract resembling consecutive arches while crossing into the contralateral protocerebral neuropil lobe (Figs. 5B, 6C, 7). Many thin neurite bundles branch off these arches in anterior direction (Figs. 5B-E, 6C-E, 7) and their additional arborizations penetrate through major parts of the protocerebral neuropil (Figs. 5D, 5E, 6D-F, 7).

From the most lateral arch of the prominent transverse tract, the “main” neurite bundle runs straight ventrally along the ascending ipsilateral DLC bundle past the oesophagus into the VNS (Figs. 5G, 6D-G, 7). Here it extends posteriorly near the midline of the VNS until thinning out by the opisthosomal neuropil (Figs. 5G, 6G, 7). It is transversely connected through punctuate SIFa-lir signal with its contralateral counterpart (Figs. 5G, 6G). Furthermore, a branch of the lateral longitudinal DMC neurite is seen splitting off and connecting to this SIFa-lir structure (Fig. 6G).

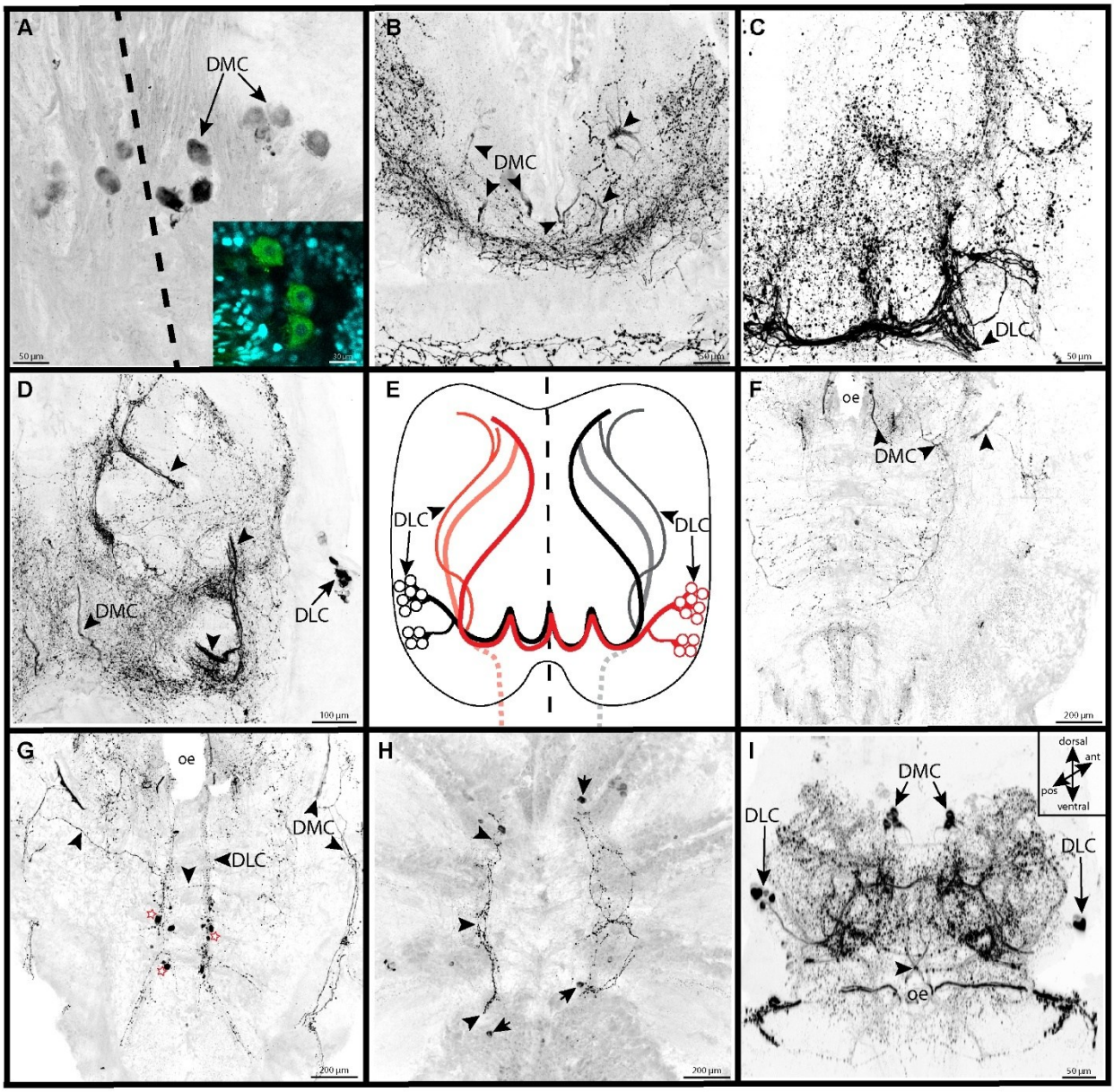

Figure 6: Details of the SIFa-lir neurons and associated VNS structures in *Cupiennius salei*. Grey-scale inverted maximum intensity projections of CLSM scans of horizontal CNS sections (**A**-**D** & **F**-**H**) or wholemounts (**I**). Arrows indicate somata, arrowheads indicate the trajectories of their neurite projections. **A.** Detail of the DMC somata. Dashed line indicates the brain midline. In the lower right corner, three of the DMCs are shown with their nuclei (SIFamide = green, nuclei = cyan). **B.** Detail of the DMC neurites as the project ventrally. **C.** Detail of one half of the transverse DLC tract. The arrowhead indicates the dorsally projecting ipsilateral DLC neurite bundle. Neurites projecting into the anterior brain neuropil belong to the contralateral counterpart. **D.** Detail of a deutocerebral hemisphere. Arrowheads depict DLC neurite bundles. The slightly darker neurite bundle indicated by the lower middle arrowhead projects from the ipsilateral DLC seen in the lateral soma cortex (arrow). Close to the midline, a DMC neurite bundle is visible. **E.** Schematic representation of the DLCs. Dorsal view. The left DLC is depicted in black, the right one in red. The lighter the shading, the more ventral is the branch innervating the brain neuropil. **F.** Detail of the DMC neurites in the VNS. The neurite bundle next to the oesophagus and the short neurite bundle sequence in the lateral deutocerebral region are connected by a

DMC neurite bundle piece in prior sections. Between these two portions, an additional neurite branches off and extends along the inner edge of the walking leg neuropils into the VNS. **G.** Collaterals branch off the anteriorly projecting DCM neurite bundle and travel the entire VNS length along the outer edge of the walking leg neuropils. Near the midline, thin DLC neurites form longitudinal tracts with commissures (middle arrowhead). Along those DLC neurites, boutons-like globular extensions can be found (stars with red outline). A thin neurite is seen connecting the outer longitudinal DMC neurite with the inner DLC tract (left arrowhead). Other thin neurites that originate from the DLCs spread through the VNS. **H.** Detail of the ventral longitudinal neurites (arrows) of unknown origin. Weakly SIFa-lir somata are located near the neurites (arrows). **I.** Extended virtual section (posterior view) of a juvenile's CNS with the DMCs and DLCs visible. Note the contralateral crossing of the DMC neurite bundles above the oesophagus (arrowhead).
Abbreviations: ant = anterior, DLC = dorsolateral neuron cluster, DMC = dorsomedial neuron cluster, oe = oesophagus, pos = posterior

<u>Weakly and/or inconsistently labelled SIFa-lir structures</u>

SIFa-lir structures in the VNS

Ventral to the longitudinal DLC tracts in the VNS, there are additional longitudinal neurites of unclear origin. They span between the boundary of the pedipalpal and first walking leg neuropils (Fig. 5I) and the end of the fourth walking leg neuropil (Fig. 6H).

In proximity of these longitudinal neurites, two to three weakly SIFa-lir somata are found in the pedipalpal and walking leg neuropils (Fig. 6H, 7), but the primary neurites of these somata could not be traced.

Likewise, there are approximately 30 other SIFa-lir somata without discernible primary neurites in the posterior half of the opisthosomal neuropil (Figs. 5H, 5I, 7).

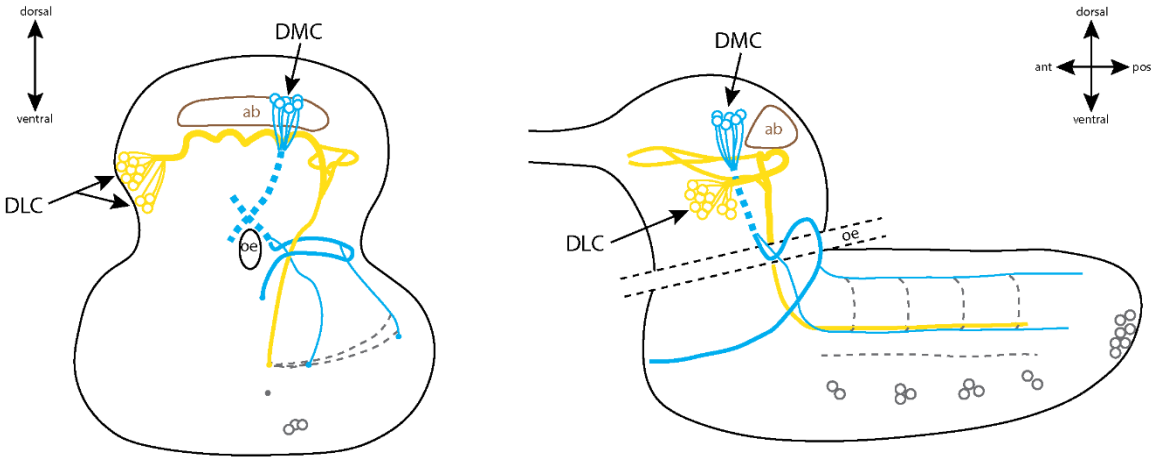

Figure 7: Schematic representations of SIFa-lir neurons and their projections in the CNS of *Cupiennius salei*. The left drawing shows an anterior view, the right shows a lateral view. Each neuron type/group is shown only for one body half (DMC – light blue, DLC – yellow, somata of the VNS – grey). Dashed grey lines indicate the SIFa-lir tracts and commissures in the VNS with uncertain origin. The blue dashed lines indicate the DMC neurite trajectories identified in the juvenile only.
Abbreviations: ab = arcuate body, ant = anterior, DLC = dorsolateral neuron cluster, DMC = dorsomedial neuron cluster, oe = oesophagus, pos = posterior

Scorpiones: *Euscorpius italicus*

Consistently labelled SIFa-lir neurons in the CNS

In each protocerebral hemisphere, three SIFa-lir dorsomedial somata are located anterodorsal to the arcuate body (Figs. 8A, 9A, 9D, 10). Furthermore, there are two weak SIFa-lir neuron clusters: a more ventral cluster in the dorsolateral protocerebral soma cortex and an anterodorsal cluster, both situated in proximity to the mushroom bodies (Figs. 8A, 9D, 10).

Ventral to the arcuate body and next to the posterolateral protocerebral neuropil, an additional weakly SIFa-lir cluster of somata is visible (Figs. 8C, 9E, 10).

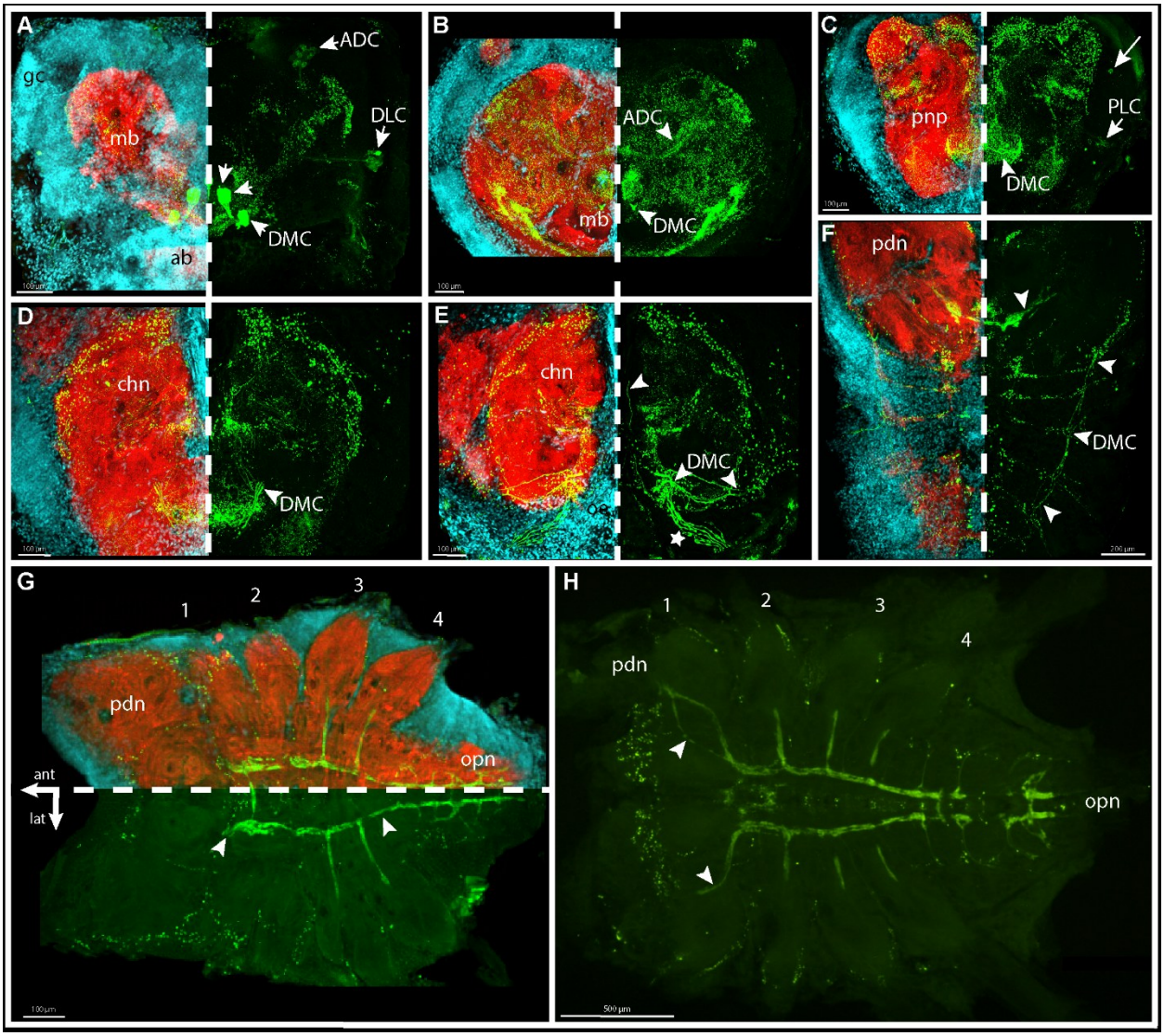

Figure 8: Overview of the SIFa-lir structures in the CNS of *Euscorpius italicus*. Maximum intensity projections of CLSM scans (**A**-**G**) and stereomicroscopic image (**H**) of horizontal vibratome sections from an adult female (**A**-**F** & **H**) and a juvenile (**G**). Apart from (**H**), the green SIFa-lir signal is shown in one image half in the context of synapsin immunolabeled structures (red) and nuclear staining (DAPI; cyan), while the other half was mirrored to show the SIFa-lir structures separately. Arrows indicate somata, arrowheads indicate their projections. **A.** Dorsal protocerebral section with the dorsomedial, anterodorsal and lateromedial neuron clusters (DMC, ADC and DLC, respectively). The DMC soma situated at the midline is part of the contralateral protocerebral hemisphere. **B.** Next protocerebral section. The ADC neurite bundles project across the mushroom bodies to the contralateral brain half, forming a shallow "W-structure". The lower arrowhead indicates the ventrally extending DMC neurites. **C.** Section near the proto- and deutocerebral boundary. The DMC neurites cross over in the posteromedian part of the protocerebral neuropil. In the lateral soma cortex, the posterolateral neuron cluster (PLC) is visible. The upper arrow marks the single SIFa-lir soma anterior to the PLC. **D.** Deutocerebral brain section (cheliceral neuropil). The DMC neurite bundle is seen right after crossing into the contralateral brain half. **E.** Brain section near the deuto- and tritocerebral (pedipalpal neuropil) boundary. The DMC neurite bundle continues to the outer edge of the cheliceral neuropil. A few collaterals are

seen branching off (star) and seem to terminate at the surface of the posterior soma cortex. A SIFa-lir neurite of unknown origin along the oesophagus resembling an element of the stomatogastric nervous system can be seen (arrowhead). **F.** Pedipalpal neuropil and the beginning of the VNS. The DMC neurites extend along the anterodorsal edge of the walking leg neuropils to the posterior end of the VNS (arrowheads). The upper middle arrowhead shows the beginning of the prominent longitudinal tract. **G.** VNS section with the SIFa-lir longitudinal tracts in the medial part of the VNS (arrowheads). In the last two walking leg neuropils, "collaterals" of this structure can be seen branching off. **H.** VNS section. The SIFa-lir longitudinal tract stretches from the pedipalpal neuropil to the opisthosomal neuropil (arrowheads).
Abbreviations: ab = arcuate body, ADC = anterodorsal neuron cluster, ant = anterior, chn = cheliceral/deutocerebral neuropil, DLC = dorsolateral neuron cluster; DMC = dorsomedial neuron cluster, gc = globuli cells, lat = lateral, mb = mushroom bodies, oe = oesophagus, opn = opisthosomal neuropil, pdn = pedipalpal/tritocerebral neuropil, PLC = posterolateral neuron cluster, pnp = protocerebral neuropil, 1-4 = walking leg neuropils

Dorsomedial neuron cluster (DMC)

Depending on the clustering of these neurons, their primary neurites run individually or as one bundle ventrally through the protocerebrum (Figs. 8A, 8B, 10). In the deutocerebral neuropil, right above the oesophagus, they cross into the contralateral brain half (Figs. 8C, 9B, 9C, 10). Along their length, many smaller neurites are branching off into the brain neuropil in anterior direction, contributing to a fine SIFa-lir network in the brain neuropil (Fig. 10). Near their crossover, the primary neurites display slightly larger, globular extensions, reminiscent of boutons (Figs. 9B, 9C). In the opposite brain half, the three neurites extend anterolaterally with additional collaterals branching off (Figs. 8C-E, 9E, 10). They then turn posteriorly and project into the VNS up to the opisthosomal neuropil, where they terminate (Figs. 8F, 9F, 10). Smaller neurites were observed branching off into the walking leg neuropils as well as into medial regions of the VNS, where they form a longitudinal varicose SIFa-lir tract, connecting the inner and outer part via commissures (Figs. 8F, 9F, 10).

Dorsolateral neuron cluster (DLC)

This cluster consists of 15 to 25 somata (Figs. 8A, 9D, 10). Its neurites travel as a bundle medially to the posterior edge of the protocerebral neuropil, where it seemingly meets its contralateral counterpart and both transition into punctuate SIFa-lir signal (Fig. 9D). This signal could not be further traced.

Anterodorsal neuron cluster (ADC)

This cluster is located anterodorsal to the mushroom body neuropil and comprises up to 30 SIFa-lir somata that show variable signal intensity, with approximately 10 of them being strongly SIFa-lir (Figs. 8A, 9D, 10). The primary neurites form a compact bundle that projects posteroventrally across the mushroom body neuropil (Figs. 8B, 10). Dorsal to the glomerular part of the mushroom bodies, the bundle crosses into the contralateral protocerebral neuropil, where it travels further ventrally (Figs. 8B, 10). From this point onwards, it was difficult to trace due to all the punctuate SIFa-lir signal in the surrounding brain neuropil. The neurites may contribute to a strongly SIFa-lir system of tracts in the VNS (Fig. 8 G, H; see below), but the "starting point" of this system is not clear either, seemingly just appearing from one section to the other.

Posterolateral neuron cluster (PLC)

In the posterolateral soma cortex, slightly dorsal to the oesophageal foramen, lies a weakly SIFa-lir neuron cluster consisting of about 20 somata (Figs. 8C, 9E, 10). The delicate primary neurites of these cells form a bundle that projects through the posterior part of the brain neuropil towards the region where the DMC neurites cross over and split off their collaterals (Fig. 9E). Owing to the prominent punctuate SIFa-lir signal in the vicinity of these DMC-associated neurites, the weakly stained PLC neurite bundle could not be traced any further with confidence. As in the case of the ADC, it therefore could not be resolved whether they potentially contribute to the prominent rope-ladder like SIFa-lir neuropilar tracts in the VNS. Anterior to the PLC, a similarly weakly stained soma can be found. Its neurite seemingly projects into the SIFa-lir brain network, yet it could not be further traced (Figs. 8C, 9E).

SIFa-lir structures in the VNS

In the pedipalpal neuromere a prominent, strongly SIFa-lir tract starts to appear (Figs. 8H, 9F, 10). No individual neurites could be distinguished and the overall dense SIFa-lir signal indicates that this tract contains quite a few synaptic connections as well.

It starts in the anterior part of the pedipalpal neuropil and splits into two posteriorly projecting branches that describe an oval shape and unite again near the posterior neuropil boundary (Fig. 8H). Close to this point, this tract is additionally connecting to its

contralateral counterpart by a SIFa-lir commissure (Figs. 8G, 8H, 9F, 10). From this point onwards, the tract runs longitudinally near the midline along the entire length of the VNS (Figs. 8G, 8H, 10). In regular intervals, a "bundle" splits off into the separate walking leg neuropils (Figs. 8G, 8H, 10). Only in the opisthosomal neuropil, the longitudinal tracts are again interconnected by commissures (Figs. 8G, 8H, 10).

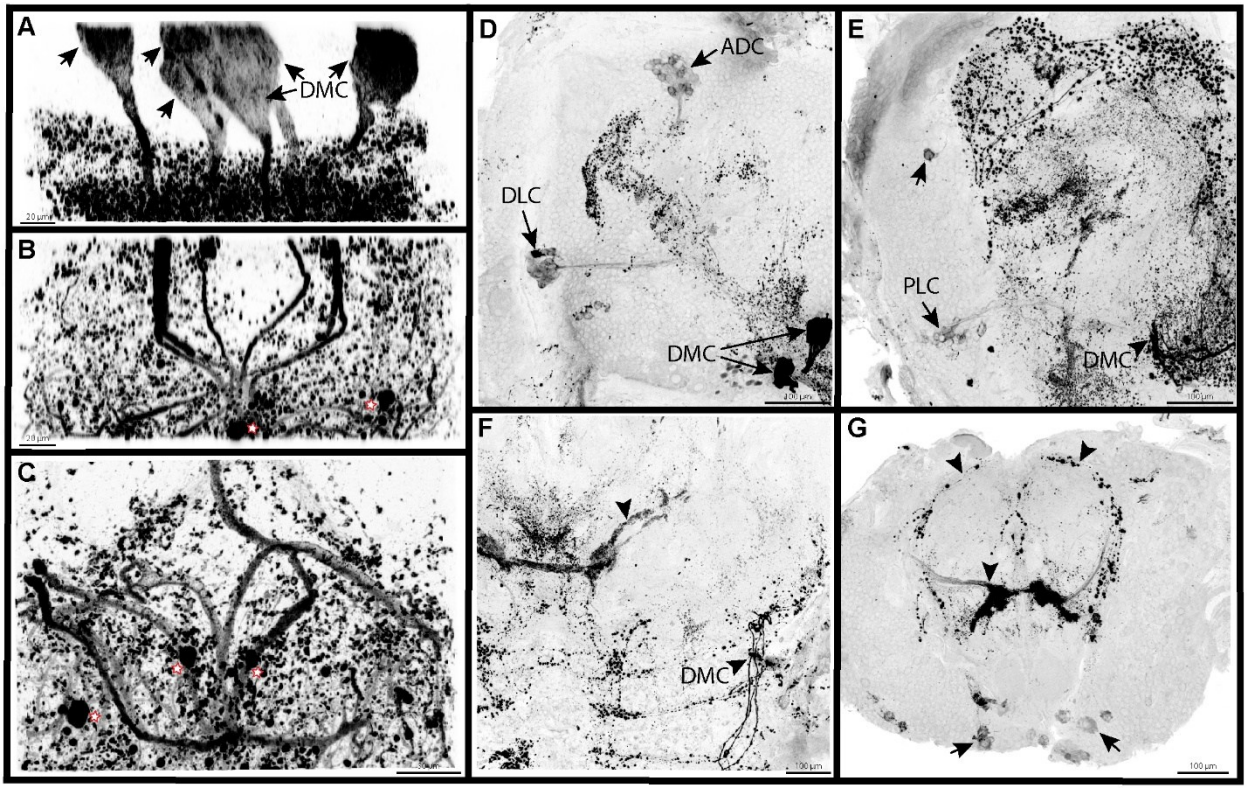

Figure 9: Details of the SIFa-lir neurons and associated VNS structures in *Euscorpius italicus*. Grey-scale inverted maximum intensity projections of CLSM scans of horizontal and cross sections (**A**-**F** and **G**, respectively). Arrows indicate somata, arrowheads indicate the trajectories of their neurite projections. **A.** Detail of the DMCs anterodorsal to the arcuate body. Two somata of each protocerebral hemisphere cluster together directly at the brain's midline. **B. & C.** Details of the crossing over of the DMC neurites from a posterolateral (**B**) and a dorsal view (**C**). Putative boutons (stars with red outline) can be seen in this region. **D.** Details of the DLC and ADC. The neurite bundles of both clusters are thin and weakly SIFa-lir. The bundle of the ADC projects ventrally whereas the bundle of the DLC travels right into the middle of a neuropil lobe, merging with a punctuate SIFa-lir domain. In the lower right corner, the DMC somata of one brain half are visible. **E.** Detail of the PLC and the anterior soma (upper arrow). In the lower left corner, the crossing over of the DMC neurites and their collaterals can be seen. **F.** Detail of the pedipalpal neuropil. The arrowhead depicts the beginning of the prominent SIFa-lir structure of the VNS. The lower arrowhead shows the projections of the DMC in the VNS. **G.** Cross section of an opisthosomal portion of the VNS. The lower arrowhead indicates the two "bundles" of the SIFa-lir structure interconnected with a commissure. Punctuate SIFa-lir signal seemingly branches off and encircles the neuropil of the VNS (upper arrowheads). In the ventral opisthosomal soma cortex, a few weak SIFa-lir somata can be found (arrows).

Abbreviations: ADC = anterodorsal neuron cluster, DLC = dorsolateral neuron cluster, DMC = dorsomedial neuron cluster, PLC = posterolateral neuron cluster

Weakly and/or inconsistently labelled SIFa-lir structures

SIFa-lir structures in the brain

One to two thin SIFa-lir neurites of unknown origin run along the anterior beginning of the oesophagus to its posterior end, resembling elements of the stomatogastric nervous system (Fig. 8E).

SIFa-lir structures in the VNS

Weak punctuate SIFa-lir signal encloses the whole neuropil region of the VNS, presumably originating from the SIFa-lir tract system, again in regular intervals (Figs. 9G, 10).

The only SIFa-lir somata in the VNS are located in the fused opisthosomal neuropil (Figs. 9G, 10). As their signal intensity was weak, tracing of their neurites was not possible.

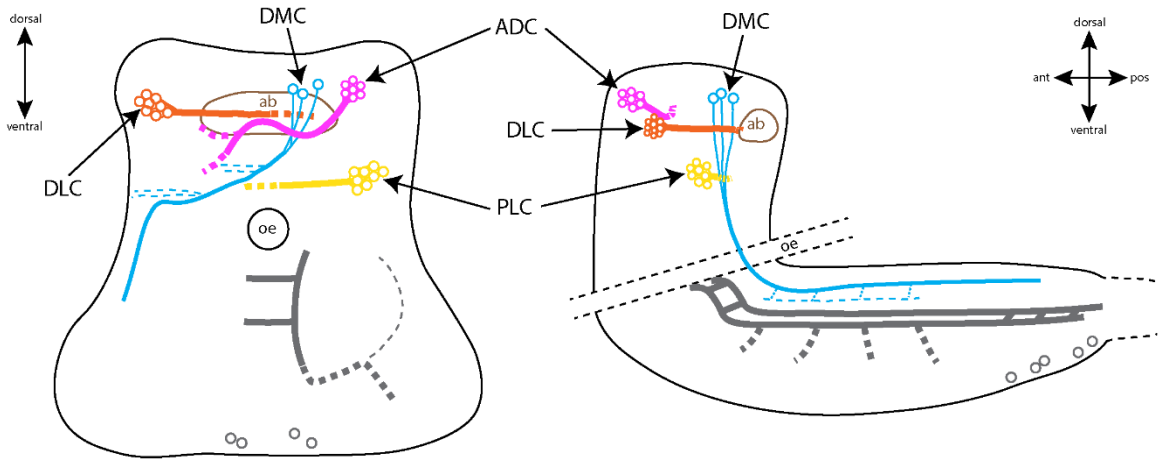

Figure 10: Schematic representations of SIFa-lir neurons and their projections in the CNS of *Euscorpius italicus*. The left drawing shows an anterior view, the right shows a lateral view. Each neuron type/group is shown for one body half only (DMC – light blue; ADC – pink; DLC – orange; PLC – yellow). Grey lines indicate the prominent system of SIFa-lir tracts and commissures in the VNS with uncertain cellular origin. Dashed lines indicate punctuate SIFa-lir patterns originating from neurites.
Abbreviations: ADC = anterodorsal neuron cluster, ant = anterior, DLC = dorsolateral neuron cluster, DMC = dorsomedial neuron cluster, oe = oesophagus, PLC = posterolateral neuron cluster, pos = posterior

Pseudoscorpiones: *Chelifer cancroides*

Consistently labelled SIFa-lir neurons in the CNS

In the proto- and upper deutocerebral soma cortex about 40 SIFa-lir somata are spread out in a complex pattern (Figs. 11A, 12A, 12D-G, 13). Only a few of these somata could be reliably identified at stereotypical positions across specimens. Anterodorsally in the protocerebral soma cortex, a cluster of five somata and their associated neurite bundles could be consistently distinguished (Figs. 11A, 11B, 12A, 12B, 12F, 12G, 13). Additional neurites are visible in the brain neuropil, but neither their origin, nor their further trajectories could be ascertained with confidence (Figs. 11-13).

Dorsal to either side of the VNS between the first and second walking leg neuropil, there is a single individually identifiable soma with strong SIFa-lir signal (Figs. 11C, 12C, 12E, 12F, 13).

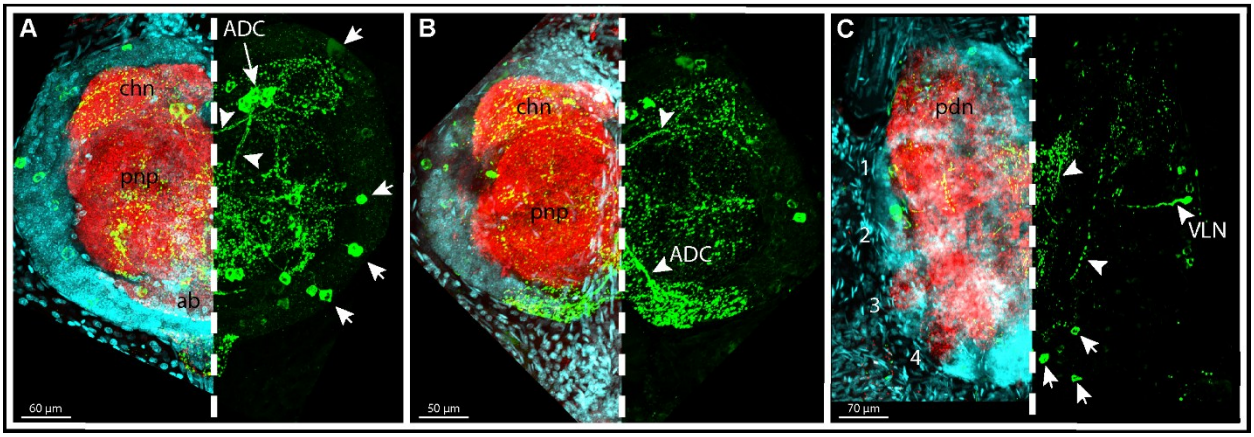

Figure 11: Overview of the SIFa-lir structures in the CNS of *Chelifer cancroides*. Maximum intensity projections (CLSM scans) of horizontal vibratome sections. The left half of each image shows SIFa-lir signal (green) in the context of synapsin-immunolabeled structures (red) and nuclear staining (DAPI; cyan). The right half shows only SIFa-lir signal. Arrows indicate somata, arrowheads indicate the trajectories of their neurite projections. **A.** First section of the brain (proto- & deutocerebrum) with the anterodorsal neuron cluster (ADC). The arrowhead underneath the cluster highlights the ventrally projecting ADC bundle whereas the arrowhead next to the ADC depicts the horizontally crossing neurite of unknown origin. The other arrows selectively mark some of the scattered proto- & deutocerebral somata. **B.** Second section of the brain (proto- & deutocerebrum). The projections of the ADC (arrowhead) terminate in the soma cortex posterior to the deutocerebral/cheliceral neuropil. The upper arrowhead indicates the horizontally crossing neurite (see **A**). **C.** Third section of the CNS (VNS) with longitudinal projections (arrowheads) and part of the neurite of the ventrolateral neuron (VLN) (arrowhead). In the opisthosomal soma cortex a few somata can be seen (arrows). *Abbreviations:* ab = arcuate body, ADC = anterodorsal neuron cluster, chn = cheliceral/deutocerebral neuropil, pdn = pedipalpal neuropil, pnp = protocerebral neuropil, VLN = ventrolateral neuron, 1-4 = walking leg neuropils

Anterodorsal neuron cluster (ADC)

The cluster consists of three large and two smaller somata (Figs. 11A, 12A, 13). It was not discernible whether the two smaller somata contribute their neurites to the main neurite bundle projecting from this cluster. The main neurite bundle travels posteriorly through the protocerebral neuropil (Figs. 11A, 12A, 12G, 13). At its centre, it projects ventrally, approaches the midline, but does not cross contralaterally (Figs. 11A, 11B, 12A, 12B, 12G, 13). It proceeds to run posterior above the oesophagus but underneath the brain neuropil (Figs. 12G, 13). Ventral to the arcuate body the neurite bundle arborizes extensively, representing a SIFa-lir domain within and beyond the outer edge of the posterior soma cortex of the brain (Figs. 11B, 12B, 12F, 12G, 13).

Ventrolateral neuron (VLN)

The soma of this neuron is located dorsolateral to the neuropil of the VNS between the first and second walking leg. Its primary neurite projects initially slightly ventrally, closer to the midline of the VNS before bending dorsally and away from the midline back towards its soma underneath the posterior end of the oesophagus (Figs. 11C, 12C, 12E, 12F, 13). From this point onwards, the varicose neurite travels dorsally along the lateral edge of the VNS before seemingly terminating around the fourth walking leg neuropil (Fig. 13).

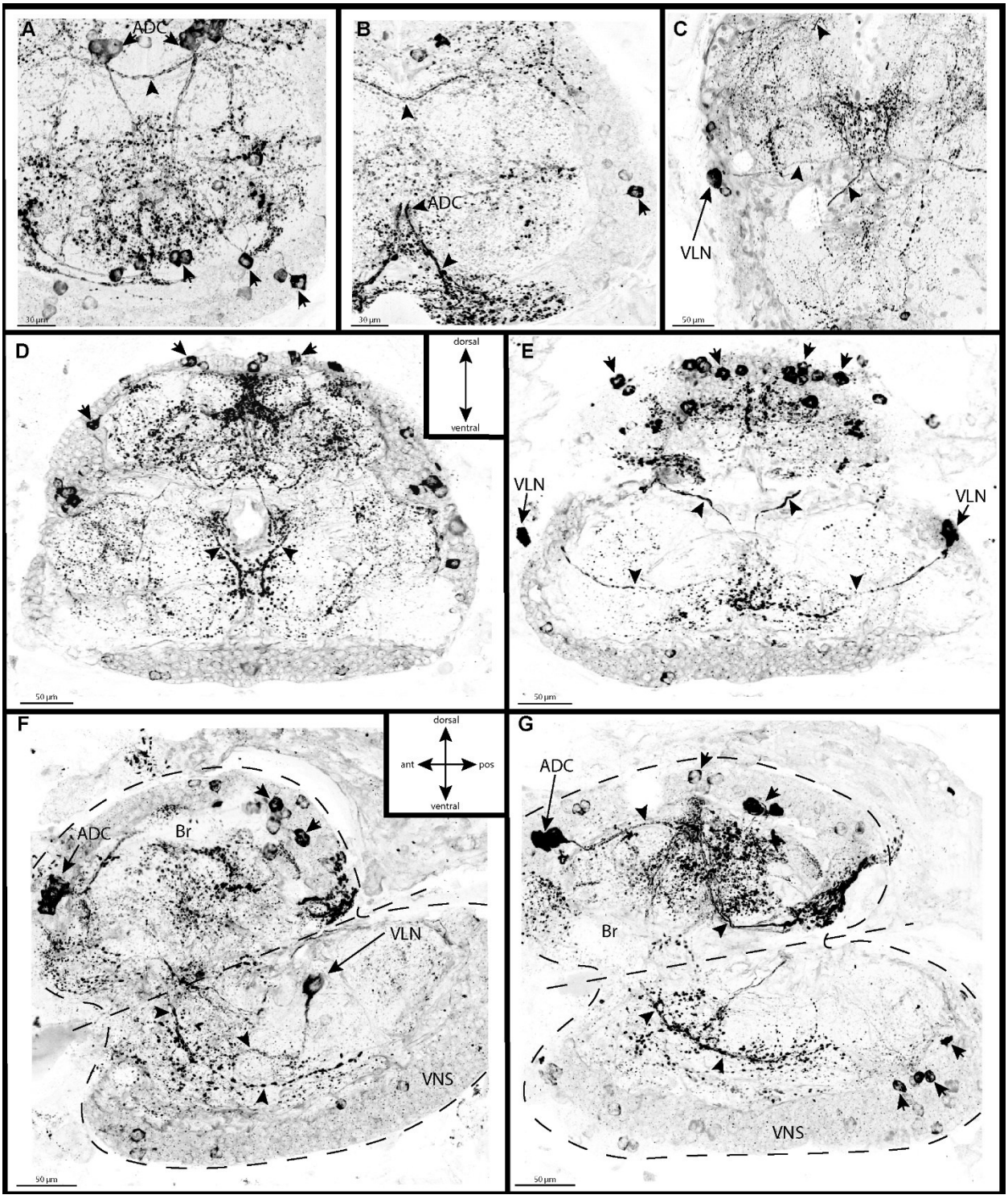

Figure 12: Details of the SIFa-lir neurons and associated VNS structures in *Chelifer cancroides*. Grey-scale inverted maximum intensity projections (CLSM scans) of horizontal (**A**-**C**), cross (**D**, **E**) and sagittal (**F**, **G**) vibratome sections. Arrows indicate somata, arrowheads indicate the trajectories of their neurite projections. **A.** Detail of the ADCs (upper arrows). The arrowhead underneath depicts the horizontally crossing neurite underneath the ADCs. Lower arrows selectively indicate other protocerebral neurons. **B.** Detail of proto- and

deutocerebrum with the termination site of the projections of the ADCs (lower arrowheads). The upper arrowhead shows the horizontally crossing protocerebral neurite. The arrow to the right highlights one of the scattered deutocerebral somata. **C.** Detail of the VLN (arrow) with its projecting neurite (arrowheads). The upper arrowhead marks the ventrally projecting neurite that formerly crossed the protocerebral neuropil underneath the ADCs. **D.** Detail of the forming longitudinal tracts along the midline of the VNS and their first commissures (arrowheads). Arrows indicate proto- & deutocerebral somata. **E.** Detail of both VLNs (arrows) and their trajectories (arrowheads). Arrows indicate proto- & deutocerebral somata. **F.** Detail of the locations of the VLN and ADC in the CNS (arrows). The dashed line indicates the outline of the CNS. Lateral view of one of the longitudinal tracts in the VNS (arrowheads; arrowhead to the right of the longitudinal tracts indicates the VLN neurite). Arrows indicate additional proto- & deutocerebral somata. **G.** Detail of the right ADC (arrow) and its complete pathway (arrowheads in the brain). The dashed line indicates the outline of the CNS. The arrowheads in the VNS depict the contralateral longitudinal tract to the one in **F**. Arrows in the brain indicate additional proto- & deutocerebral somata, arrows in the VNS depict opisthosomal somata.
Abbreviations: ADC = anterodorsal neuron cluster, ant = anterior, Br = brain, pos = posterior, VLN = ventrolateral neuron, VNS = ventral nervous system

Weakly and/or inconsistently labelled SIFa-lir structures

Posteroventral to the ADC, what seems to be one or even two SIFa-lir neurites stretch transversely through the protocerebral neuropil (Figs. 11A, 11B, 12A, 12B, 13). While the soma or somata giving rise to this neurite/these neurites could not be identified, they are likely to originate in the proto- or deutocerebrum as this neurite/these neurites project into the VNS, where varicose SIFa-lir signal connects the neurite/these neurites to a weakly stained longitudinal tract running in parallel to a medial “rope-ladder”-like tract system (Fig. 12C, 13).

SIFa-lir structures in the VNS

The “rope-ladder”-like tracts are interconnected by commissures in the middle (Figs. 11C, 12C, 12D, 12F, 12G, 13). The varicose SIFa-lir tract presumably originating from the before mentioned protocerebral neurite/neurites is seemingly connected to the middle tracts (Figs. 12C, 13). Both structures end at the opisthosomal neuropil (Figs. 11C, 12C, 12F, 12G, 13).

In the ventral opisthosomal soma cortex, a few SIFa-lir somata are present (Figs. 11C, 12C, 12F, 12G, 13). As in the case of most of the SIFa-lir somata in the protocerebrum, their neurites were stained too weakly to enable confident tracing. However, some somata appear to send projections towards the neurite tracts along the midline of the VNS (Fig. 12C).

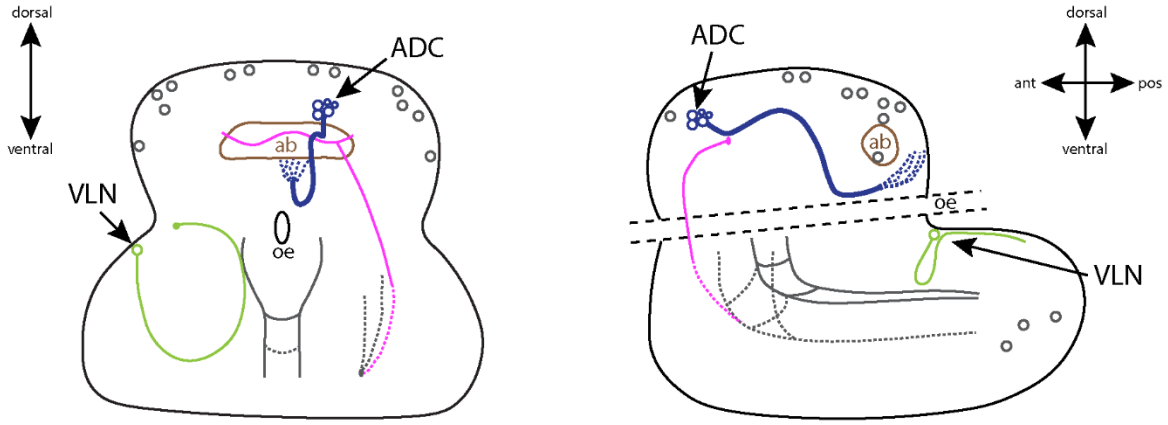

Figure 13: Schematic representations of SIFa-lir neurons and their projections in the CNS of *Chelifer cancroides*. The left drawing shows an anterior view, the right shows a lateral view. Each neuron type/group is shown only for one body half (ADC – dark blue; VLN – light green; horizontally crossing neurite – pink). Dashed lines indicate punctuate SIFa-lir patterns originating from neurites. Dashed grey lines show weakly SIFa-lir neurite projections in the VNS. Grey lines indicate the SIFa-lir tracts and commissures in the VNS with uncertain origin.
Abbreviations: ab = arcuate body, ADC = anterodorsal neuron cluster, ant = anterior, oe = oesophagus, pos = posterior, VLN = ventrolateral neuron

Solifugae: *Rhagodes* sp.

Consistently labelled SIFa-lir neurons in the CNS

In each protocerebral hemisphere, there are four dorsal somata (Figs. 14A, 15A, 16). One cluster of three somata is located in the medial part of the protocerebrum, anterodorsal to the arcuate body. The fourth soma can be found anterior to this cluster, positioned between the globuli cells of the mushroom bodies (Fig. 14A, 16).

In addition to these dorsal somata, there is a dorsolateral cluster of tightly packed somata lateral to the mushroom bodies (Figs. 14A, 15B, 16).

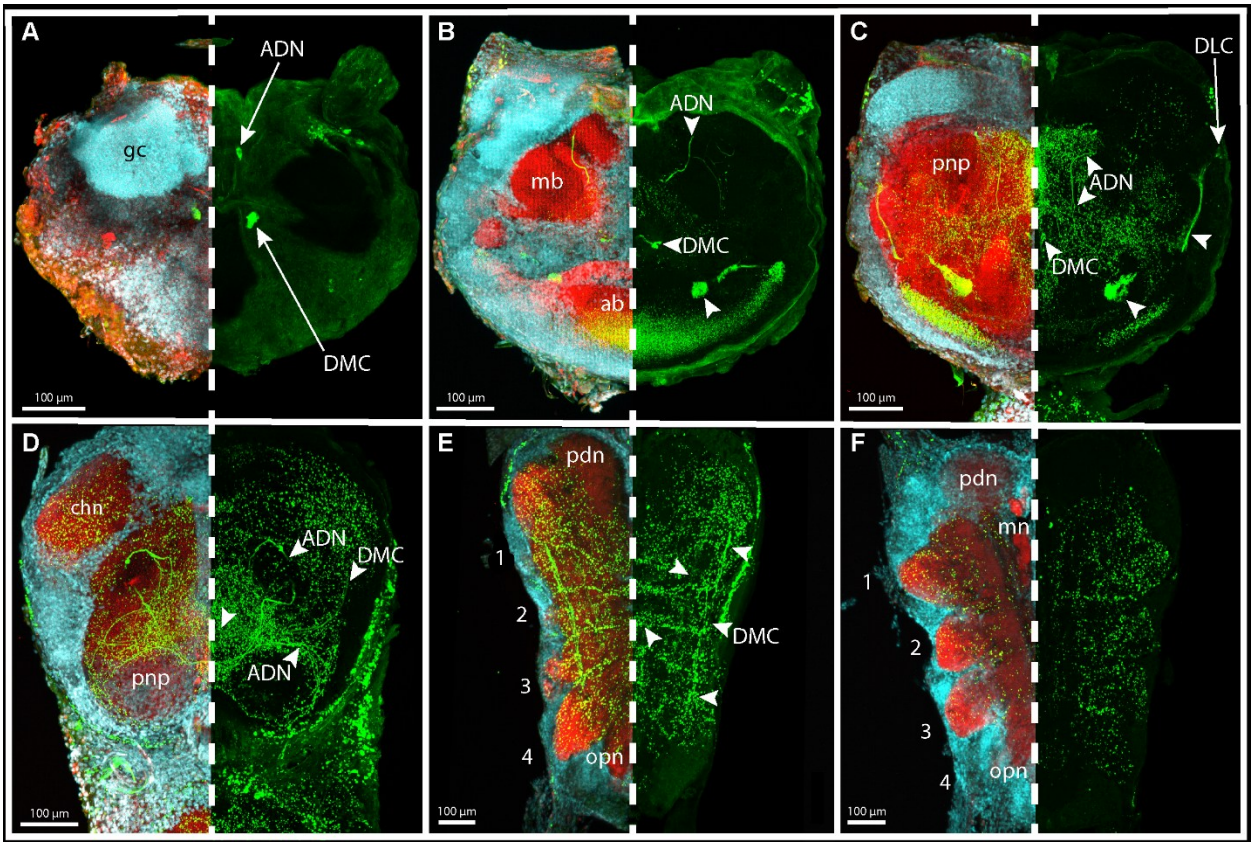

Figure 14: Overview of SIFa-lir structures in the CNS of *Rhagodes* sp. Maximum intensity projections of horizontal vibratome sections proceeding from dorsal to ventral. The left half of each image shows SIFa-lir (green) in the context of synapsin immunolabeled structures (red) and nuclear staining (DAPI; cyan). The right half shows only SIFa-lir. Arrows indicate somata, arrowheads indicate the trajectories of their neurite projections. **A.** First section of the brain (protocerebrum) with the somata of the dorsomedial neuron cluster (DMC) and the single anterodorsal neuron (ADN). **B.** Second section of the brain (protocerebrum) with ventrally projecting neurites of the DMC and ADN. First indications of the tear drop-shaped, strongly SIFa-lir neuropilar domain of the dorsolateral neuron cluster (DLC) can be seen slightly anteroventral to the arcuate body (arrowhead). **C.** Third section of the brain (protocerebrum) with the DLC and its posteriorly projecting neurite bundle that ends in this SIFa-lir neuropilar domain ventral to the arcuate body (arrowhead). **D.** Fourth section of the brain (proto- & deutocerebrum/cheliceral neuropil). The DMC neurite bundle crosses contralaterally and projects towards the periphery of the brain neuropil. The ADN neurite extends ventrally before coming back up to cross contralaterally and ending in the opposite brain hemisphere. **E.** Fifth section of the brain (tritocerebrum/pedipalpal neuropil) and the VNS. The DMC neurite bundle runs along the outer edge of the walking leg neuropils (arrowheads) and are transversely interconnected by punctuate SIFa-lir neurite staining (middle arrowhead). Note the weakly SIFa-lir longitudinal tracts medial to the DMC neurite bundle (arrowhead between the midline and the lateral DMC bundle). **F.** Sixth section of the VNS. Diffuse punctuate SIFa-lir signal is present along the edges of the walking leg neuromeres.

Abbreviations: ab = arcuate body, ADN = anterodorsal neuron, chn = cheliceral/deutocerebral neuropil, DLC = dorsolateral neuron cluster, DMC = dorsomedial neuron cluster, gc = globuli cells, mb = mushroom bodies, mn = malleolar neuropil, opn = opisthosomal neuropil, pdn = pedipalpal/tritocerebral neuropil, pnp = protocerebral neuropil, 1-4 = walking leg neuropils

Dorsomedial neuron cluster (DMC)

Three primary neurites emanate from the DMC and form a ventrally projecting neurite bundle (Figs. 14B, 15A, 16). This bundle runs anterior to the arcuate body through the protocerebral brain neuropil and subsequently converges with its contralateral counterpart (Figs. 14B-D, 15C). Right above the oesophagus, it crosses contralaterally, proceeds in a lateral direction along the posterior edge of the brain neuropil, and then extends to a more anterior region of the contralateral brain half (Figs. 14D, 15C, 16). From this point onwards, the bundle bends posteriorly and runs dorsally along the entire length of the VNS (Fig. 14E, 16). At regular intervals, the longitudinal neurite bundles of both body halves are transversely connected by punctuate SIFa-lir signal, likely representing commissural tracts of the walking leg neuropils (Fig. 14E, 16).

Anterodorsal neuron (ADN)

The neurite of the ADN travels also ventrally (Figs. 14A, 15A, 16). While small neurites branch off in posterior direction to innervate the central brain neuropil, the "main" neurite runs past the oesophagus (Figs. 14B-E, 15C, 16). After reaching the deutocerebral neuropil, it bends back up and projects posteriorly, passing the neurite bundle of the DMC laterally (Figs. 14D, 15C, 16). It then turns medially and meets its contralateral counterpart as it crosses into the other brain half (Figs. 14D, 15C, 16). Here, it terminates in a semi-circular loop within a neuropil lobe located dorsolateral to the oesophagus and ventral to the arcuate body (Figs. 14D, 15C, 16).

Dorsolateral neuron cluster (DLC)

This cluster, consisting of approximately 15 to 20 somata, is situated in the outer soma cortex next to the mushroom bodies (Figs. 14C, 15B, 16). Their neurites form a bundle that extends horizontally along the outer edge of the mushroom body neuropil to the posterior half of the brain (Figs. 14C, 15B, 16). It then projects medially, where it terminates as a tear drop-shaped strongly SIFa-lir neuropilar domain. (Figs. 14B, 14C, 16).

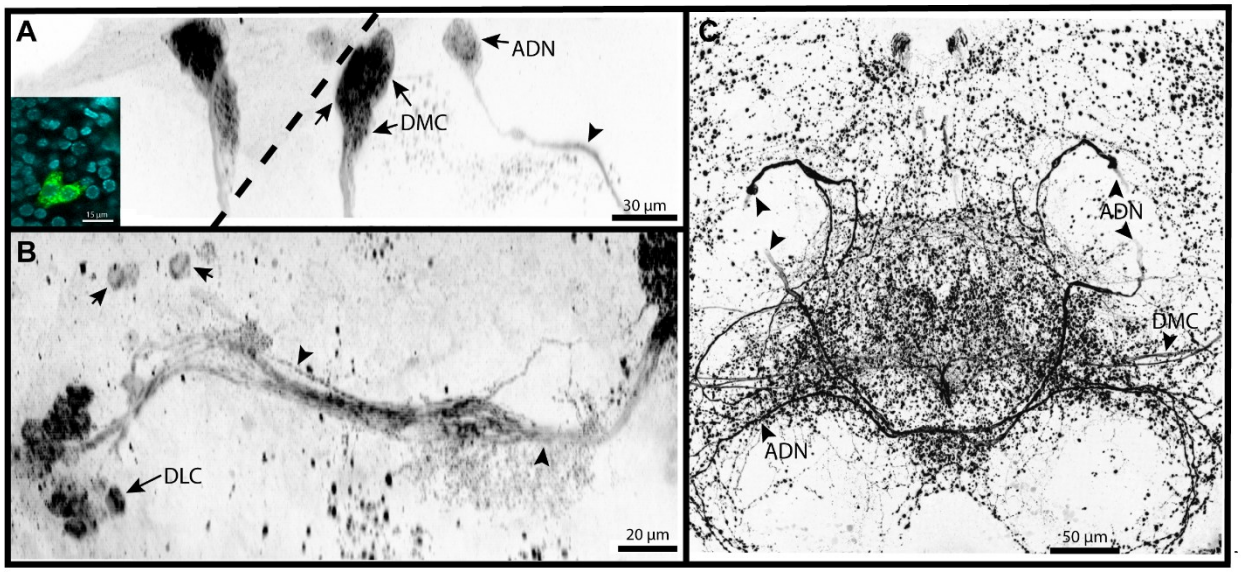

Figure 15: Details of the SIFa-lir protocerebral neurons (grey-scale inverted). Arrows indicate somata, arrowheads indicate the trajectories of their neurites. **A.** DMC and ADN of both brain hemispheres seen from a diagonal posterior view (dashed line). Arrows indicate the separate neuronal somata. In the lower left corner, two of the DMCs shown with their nuclei (SIFamide = green, nuclei = cyan). **B.** Left DLC with its neurites projecting to the posterior part of the brain from a lateral view. Arrow indicates the cluster that gives rise to a neurite bundle toward to posterior-medial protocerebrum. Note four weakly stained somata (arrows) dorsal to the cluster with neurites that also converge with the neurite bundle. In the upper right corner dense SIFa-lir from the arcuate body can be seen. **C.** Detail of the ADN projections and their crossing over as well as the DMC projections (right arrowhead), which previously crossed over and are now running to each edge of the contralateral protocerebral neuropil (out of frame).
Abbreviations: ADN = anterodorsal neuron, DLC = dorsolateral neuron cluster, DMC = dorsomedial neuron cluster

Weakly and/or inconsistently labelled SIFa-lir structures

SIFa-lir structures in the brain

Additionally, some weakly labelled SIFa-lir somata were observed in the soma cortex anterior to the protocerebral neuropil. However, they differed in size and number in the two individuals studied and their neurites could not be traced with certainty. The identification of thin neurite bundles running posteriorly along the oesophagus as belonging to these anterior somata awaits confirmation in future studies.

SIFa-lir structures in the VNS

In contrast to the dorsal portion of the VNS, there is only diffuse SIFa-lir signal in its ventral portion, being found throughout and along the edges of the walking leg and opisthosomal neuropils. However, there are weakly SIFa-lir longitudinal tracts running parallel to the DMC neurite bundle close to the VNS midline (Figs. 14E, 16), but their origins were not traceable in the specimens studied.

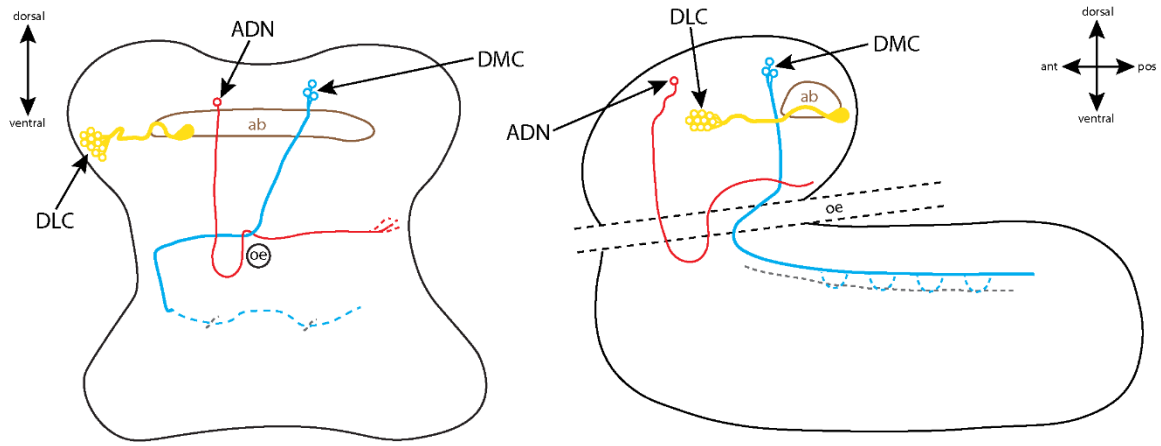

Figure 16: Schematic representations of SIFa-lir neurons and their major projections in the CNS of *Rhagodes* sp. The left drawing shows an anterior view, the right shows a lateral view. Each neuron type/group is shown only for one body half (DMC – light blue; ADN – red; DLC – yellow). Dashed lines indicate punctuate SIFa-lir patterns originating from neurites. Dashed grey lines show weakly SIFa-lir longitudinal tracts in the VNS. *Abbreviations*: ab = arcuate body, ADN = anterodorsal neuron, DLC = dorsolateral neuron cluster, DMC = dorsomedial neuron cluster; oe = oesophagus

Discussion

Brief recap of phylogenetic debates revolving around the taxa studied

The phylogenetic relationships between the 13 extant euchelicerate orders are still under debate (see Brusca et al., 2023; Gainett et al., 2024; Nolan et al., 2020 for collected phylogenetic data) (Fig. 17). Despite ongoing discussions, however, at least some of the extant orders are by now widely recognized to form monophyletic groups within the euchelicerate tree. This holds for Tetrapulmonata, consisting of spiders, amblypygids (whip spiders), uropygids (whip scorpions) and schizomids (small whip scorpions), which reliably

cluster together in both morphological and molecular analyses (e.g. Ballesteros et al., 2019; Gainett et al., 2024; Nolan et al., 2020; Sharma & Gavish-Regev, 2024).

Aside from the Tetrapulmonata another clade has gotten phylogenetic support through recent molecular studies, which places scorpions and pseudoscorpions as sister groups to each other (Ballesteros et al., 2022; Gainett et al., 2024; Ontano et al., 2021). While the placement of scorpions as the sister group to the tetrapulmonates has been consistently recovered in molecular phylogenetic studies, forming the Arachnopulmonata (Nolan et al., 2020; Regier et al., 2010; Sharma et al., 2014), the placement of pseudoscorpions is much more debated. Recently, Ontano et al. (2021) recovered pseudoscorpions as the sister group to scorpions, with which they share extensive gene duplications in the genome that are also characteristic of the tetrapulmonate taxa. The “extended” Arachnopulmonata hypothesis therefore advocates Panscorpiones (scorpions + pseudoscorpions) as the sister group to Tetrapulmonata (Ballesteros et al., 2022; Brusca et al., 2023; Gainett et al., 2024; Ontano et al., 2021). Under this hypothesis, the name-giving book lungs of arachnopulmonates must have been secondarily lost in the pseudoscorpions, as one of the classical apulmonate taxa.

Beyond arachnopulmonates, this study also focused on the neuronal projections of solifuges, which still do not have a robustly supported position in the phylogenetic tree (Brusca et al., 2023; Gainett et al., 2024). Solifuges were previously proposed to be the sister group to pseudoscorpions based on morphological data, which stands opposed to more recent molecular data (Gainett et al., 2024). In molecular tree topologies, solifuges are variably recovered in a close relationship to either Ricinulei, Palpigrada or Acariformes (e.g. Ballesteros et al., 2019; Ballesteros et al., 2022; Regier et al., 2010). These relationships are believed to be further reinforced by shared morphological characteristics, albeit it in most of the discussed alternatives just one character, for instance the shared morphology of the coxal gland in solifuges and palpigrades or a specific ventral division of the prosoma found only in solifuges and Acariformes (Gainett et al., 2024).

Homologous SIFa-lir neurons in the brain of Tetrapulmonata

The SIFa-lir neurons of the spider *Cupiennius salei* and the three amblypygid species studied show several striking similarities, which support their interpretation as a homologous neuron type (Fig. 17). Apart from the similar soma position in the protocerebrum, the DMC/DPC main neurites show the same trajectory, crossing contralaterally before descending into the VNS and extending longitudinally along its entire length. One difference between the spider DMCs and amblypygid DPCs lies in their neuron number. There are three neurons in the amblypygids but six neurons in the spider. In addition to the three neurites forming this specific descending pathway, the remaining DMC neurites of the spider project differently and innervate other regions of the CNS, including the efferent pedipalpal nerve (Fig. 17). These differences likely represent taxon-specific modifications. In addition to the DMC/DPC, also the neurite bundles of the lateral protocerebral DLCs descend in both tetrapulmonate taxa into the VNS along the midline until the opisthosomal neuropil. The only difference is that the DLCs in *C. salei* cross contralaterally in the protocerebrum before projecting ventrally whereas the equivalent clusters of all three amblypygids stay ipsilateral while projecting ventrally (Fig. 17). Despite this deviation, the DLCs of both orders are here tentatively proposed to be homologous. However, to enable a more informed evaluation of this issue, especially regarding potential lineage-specific modifications, further studies on Thelyphonida (uropygids + schizomids), the sister group to amblypygids should be conducted.

Additional support for Panscorpiones from SIFa-lir neuron patterns?

Compared to the tetrapulmonates studied, the scorpion *Euscorpius italicus* and the pseudoscorpion *Chelifer cancroides* display noticeably more SIFa-lir neuronal somata in the brain, especially in the protocerebrum (Fig. 17). In general, both *E. italicus* and *C. cancroides* show a larger proportion of speckled SIFa-lir neuropilar domains in the brain, but for the most part, these domains could unfortunately not be confidently associated with neuronal somata or their projections. This restricts the conclusions that can be drawn on the cell level. The same applies to the “rope-ladder”-like SIFa-lir tract system in the VNS of both taxa.

Especially in the scorpion, this structure exhibits strong SIFa-lir signal and it is surprising that no neuronal somata could be confidently assigned in any of the specimens investigated.

However, a unique feature shared by scorpion and pseudoscorpion is a transversally crossing, w-shaped neurite or neurite bundle in the anterior protocerebrum underneath the ADCs (pseudoscorpion) or anteroventrally to the DMCs (scorpion) (Fig. 17). While these neurites originate from the ADCs in *E. italicus*, their further trajectories could not be traced. By contrast, the situation in *C. cancroides* is the other way around, as the neuronal somata remain currently unknown (Fig. 17). Pending a better resolution of the respective missing elements in both taxa, a set of SIFa-lir protocerebral neurons with these prominent, uniquely shaped commissural neurite pathways may be revealed as a putative synapomorphy in support of scorpions and pseudoscorpions as sister groups.

In *E. italicus* the DMC neurites project contralaterally above the oesophagus, descend into the VNS and project posteriorly, closely mirroring the pattern of DMC/DPC neurons in the amblypygids and the spider (Fig 17). Hence why the scorpion DMC neurons are proposed to be homologous to the amblypygid DPC neurons and the spider DMC neurons (Fig 17). Furthermore, the PLCs in the scorpion resemble the tetrapulmonate DLCs in their position, however due to the inability to trace the PLC neurites, it is not possible to fully homologize them.

In contrast, the ADC neurites of *C. cancroides* project completely differently to any of the DMCs/DPCs or other arachnopulmonate neuron clusters, as they do not descend into the VNS but terminate in the brain (Fig. 17). Interestingly, they arborize into a domain of varicose SIFa-lir signal not only underneath the arcuate body, but also outside of the brain neuropil, even beyond the posterior soma cortex (Fig. 17). A possible explanation could be that the ADCs are associated with the circulatory system. The heart and the CNS of pseudoscorpions, or all apulmonate taxa, are connected via the aorta, which “opens” into a thin interstitial space that surrounds the CNS, the perineural vascular membrane (Firstman, 1973). This transition between aorta and perineural vascular membrane is located on the posterior side of the brain (Firstman, 1973), right where the punctuate SIFa-lir signal can be

found. Accordingly, these SIFa-lir dots could mark a site where vesicles containing SIFamide are released into the hemolymph within the perineural vascular membrane and further into the circulatory system. This could mean that SIFamide has a neurosecretory function. However, additional studies are needed to corroborate this hypothesis.

In addition to the ADCs, a single SIFa-lir soma can be seen in the VNS near the border between brain and VNS, which is more intensely labelled and bigger than the somata in the VNS soma cortex (Fig. 17). Weakly SIFa-lir somata can be observed in the ventral soma cortex of all arachnopulmonates, but their neurite projections could be rarely traced (Fig. 17). By contrast, the VLN of *C. cancroides* is strongly SIFa-lir and projects dorsally into the VNS (Fig. 17). Together with the ADC pattern, these SIFa-lir neurons seem to be characteristic – and thus potentially autapomorphic – for pseudoscorpions and cannot be found in any of the other species investigated (Fig. 17).

SIFa-lir neurons in the solifuge – another chance for Haplocnemata?

Some features of the SIFa-lir pattern in the solifuge *Rhagodes* sp. bear notable resemblances to the arachnopulmonates (to the exclusion of pseudoscorpions) (Fig. 17). For instance, the solifuge DMCs represent descending neurons that project into the contralateral half of the VNS, where their projection shows minor differences (Fig. 17). While the "rope-ladder"-like domain in the VNS of the tetrapulmonates is formed by the DLCs, in the solifuge this structure is made by the DMCs (Fig. 17). Additionally, also *Rhagodes* sp. has a prominent DLC, which ends in a dense neuropilar domain underneath the arcuate body (Fig. 17). This is the main difference between the solifuge and the two tetrapulmonate taxa studied, in which the DLCs are descending neurons (Fig 17). Since the SIFa-lir signal of the scorpion DLCs could not be further traced in the brain neuropil, a more detailed comparison between the scorpion and solifuge DLCs is currently not possible. However, based on the position of the DLCs in the solifuge, they can be cautiously deemed as potential homologs to the arachnopulmonate DLCs, assuming that their termination site in the solifuge brain is a taxon-specific modification (Fig. 17). Contrasting to this, it is evident that the SIFa-lir patterns of the solifuge and the pseudoscorpion do not share striking similarities (Fig. 17). The only potential commonality could be the punctuate SIFa-lir signal found also in the

perineural vascular membrane of the apulmonate solifuge. However, it is more scattered and associated neurons could not be determined. Furthermore, without looking into other apulmonate chelicerate taxa, it cannot be ruled out that this signal is a common feature for all apulmonates. Accordingly, the neuron patterns described in this study do not support for the traditional Haplocnemata hypothesis (Solifugae + Pseudoscorpiones), which is increasingly challenged by molecular datasets.

Figure 17 (next page): Comparison of the proposed homologous SIFa-lir neurons of the taxa studied. The schematic drawings (anterior view) are shown in the context of the currently favoured hypothesis of chelicerate phylogeny based on Brusca et al. (2023) [left lower corner]. Dashed lines of the phylogenetic tree indicate other branches. The neuron types proposed to be homologous are shown in corresponding colours, whereas additional neurons without clear counterparts in other taxa are shaded in grey. The characteristic projection of the DMCs/DPCs (light blue) can be seen in all taxa except for the pseudoscorpion. Apart from the latter, all taxa display also a lateral cluster (yellow), but with differing target site. The scorpion ADCs and the horizontally crossing neurite of the pseudoscorpion are present only in the Panscorpiones (magenta).
Abbreviations: ab = arcuate body, oe = oesophagus

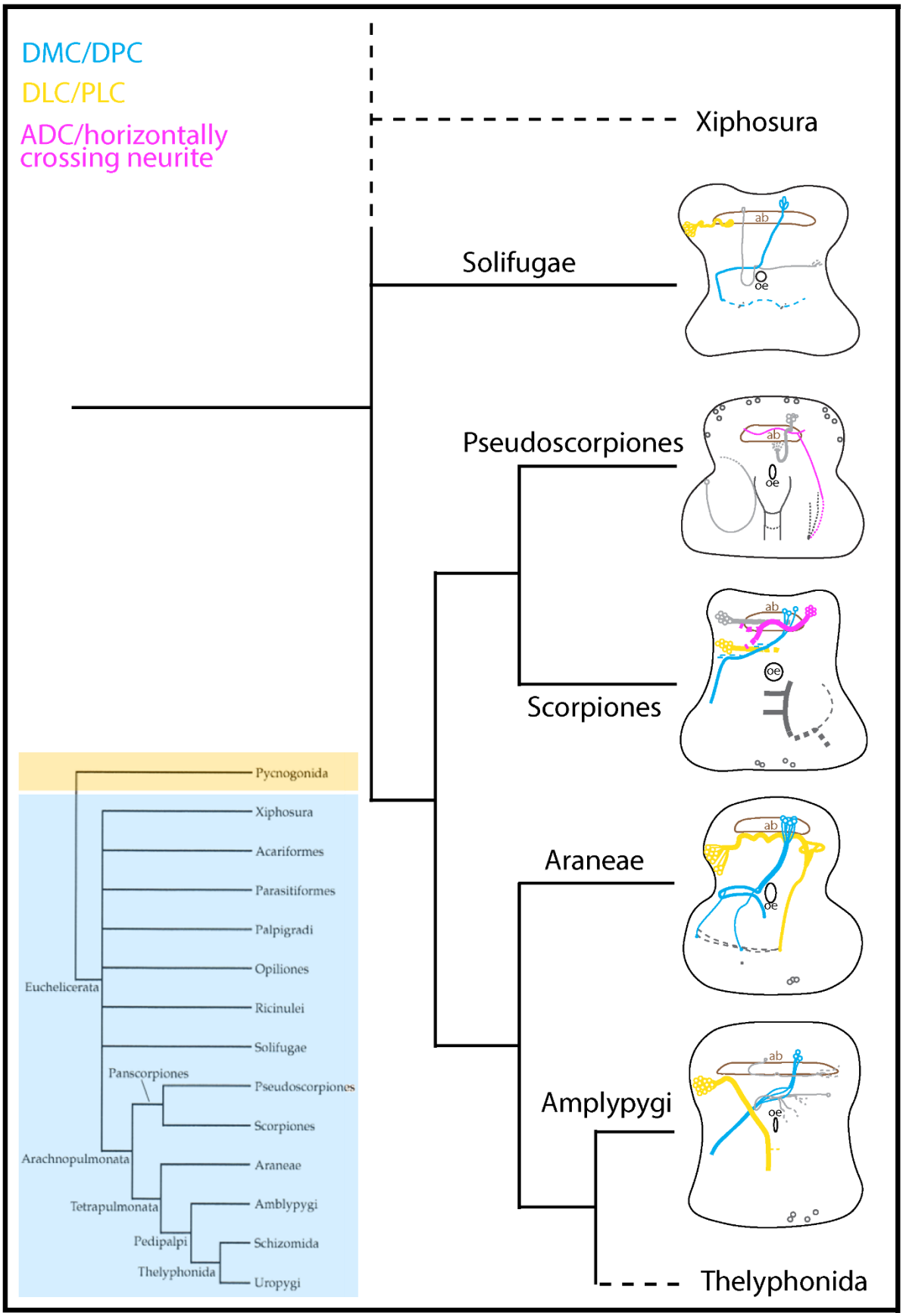
DMC/DPC
DLC/PLC
ADC/horizontally crossing neurite
Xiphosura
Solifugae
Pseudoscorpiones
Scorpiones
Araneae
Amplypygi
Thelyphonida
ab
oe
Pycnogonida
Xiphosura
Acariformes
Parasitiformes
Palpigradi
Opiliones
Ricinulei
Solifugae
Pseudoscorpiones
Scorpiones
Araneae
Amblypygi
Schizomida
Uropygi
Panscorpiones
Arachnopulmonata
Tetrapulmonata
Pedipalpi
Thelyphonida
Euchelicerata

SIFa-lir neurons in the CNS of other euchelicerate taxa

This study originally aimed to also provide insights into SIFa-lir neurons of Xiphosura (horseshoe crabs), given their contentiously debated phylogenetic position (Ballesteros & Sharma, 2019; Howard et al., 2020; Nolan et al., 2020). However, owing to significant delays in the delivery of *Limulus polyphemus* specimens, only preliminary data could be obtained, calling for future investigations in more detail.

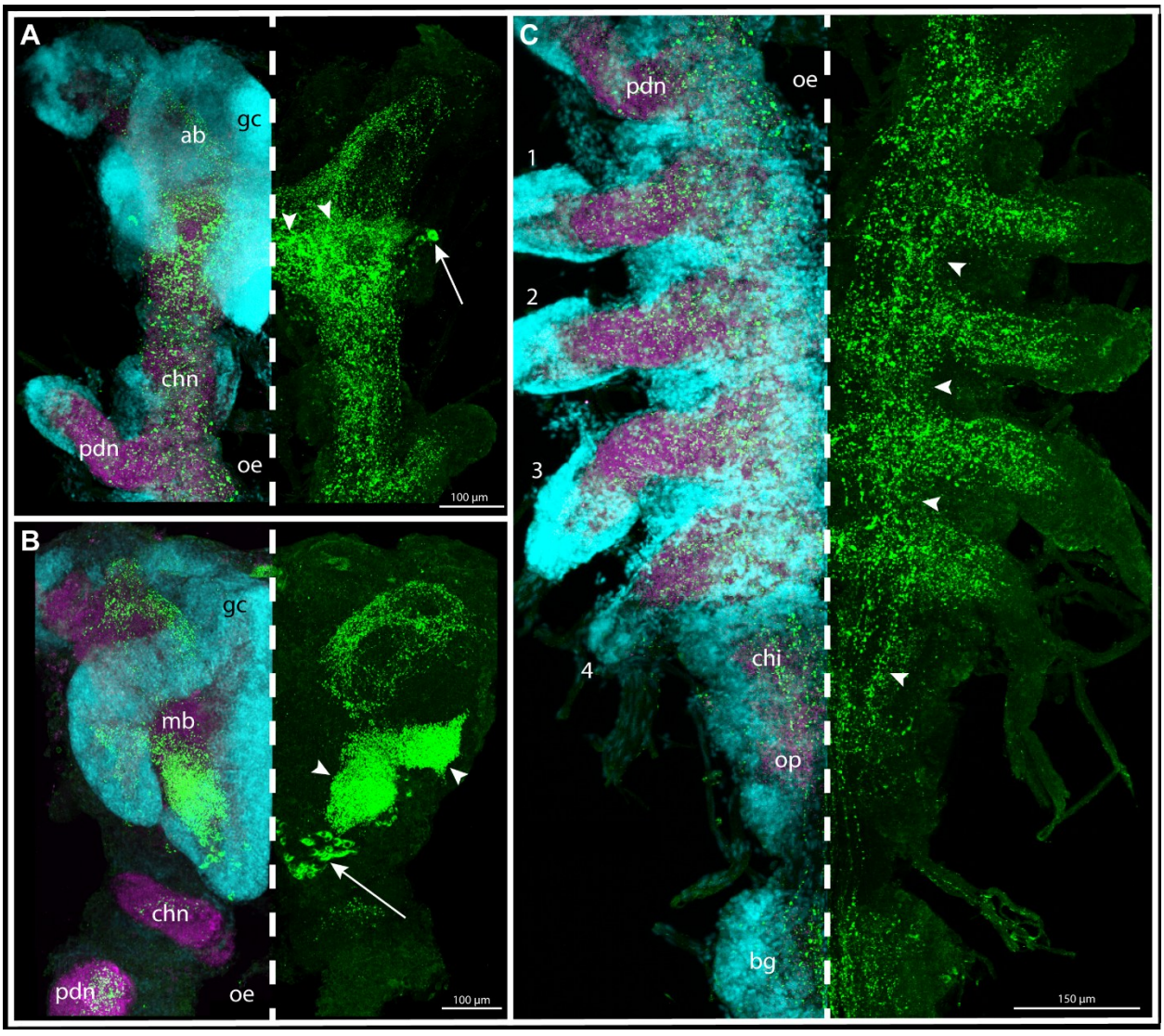

Figure 18: Preliminary data the SIFa-lir structures in the CNS of *Limulus polyphemus*. Maximum intensity projections of CLSM scans of juvenile wholemounts (**A**, **C**) and a horizontal vibratome section of a juvenile brain (**B**). The green SIFa-lir signal is shown in one image half in the context of synapsin immunolabeled structures (magenta) and nuclear staining (DAPI; cyan), while the other half only shows SIFa-lir signal. Arrows indicate

somata, arrowheads indicate their projections. **A.** Wholemount of the brain. In the lateral soma cortex posterior to the arcuate body, a soma can be seen (arrow). Moreover, varicose SIFa-lir signal is visible throughout the brain neuropil. In the median part of the protocerebrum a diffuse SIFa-lir commissural domain can hardly be detected (arrowheads). **B.** Ventral brain section. Strong SIFa-lir signal is visible in the most ventral lobes of the mushroom bodies (arrowheads). Dorsoposterior to the mushroom bodies a cluster of more than a dozen somata with unclear projections is highlighted (arrow). **C.** VNS. Longitudinal SIFa-lir tracts stretch across the entire length of the VNS (arrowheads).
Abbreviations: ab = arcuate body, bg = book gill ganglia, chi = chilaria, chn = cheliceral/deutocerebral neuropil, gc = globuli cells, mb = mushroom bodies, oe = oesophagus, op = operculum, pdn = pedipalpal/tritocerebral neuropil, 1-4 = walking leg neuropils

Based on the preliminary data, it is evident that also the brain of *L. polyphemus* exhibits regions of strong SIFa-lir signal, among others in parts of the arcuate body and the mushroom bodies (Fig. 18A, B). However, at the available resolution only few individual somata could be confirmed and the tracing of their neurites is challenging (Fig. 18). In the VNS, longitudinal neurites with varicosities are visible reaching at least to the book gill ganglia (Fig. 18C). Speckled SIFa-lir signal is also seen in the walking leg neuropils as well as forming commissures between them (Fig. 18C).

The only other study on SIFa-lir neurons in the euchelicerate CNS focused on the black-legged tick *Ixodes scapularis* (Šimo et al., 2009; Šimo et al., 2013). Corresponding to the results of the present study, they found various single and clustered SIFa-immunoreactive neuronal somata in stereotypical positions within the CNS. Most prominently among them is one giant neuron per posterior protocerebral lobe that projects into the pedipalpal nerve and further into the salivary nerve, where it arborizes and innervates the salivary glands. Additionally, four neurons located in the ventromedial part of each protocerebral hemisphere were found which projected into the VNS (Šimo et al., 2009). The projection pathway of the giant neurons is in particular reminiscent of the DMC pathway in the spider, which includes a subset of efferent neurites that likewise project into the pedipalpal nerve. Interestingly, the ventromedial protocerebral neurons of the tick and one of the DMC neurites of the spider resemble each other in their longitudinal projections in the VNS, in

which they travel along the inner edge of the walking leg neuropils and terminate near the fourth walking leg/opisthosomal neuropil border. However, the neurites of both neuron types in the tick seem to remain ipsilateral (Šimo et al., 2009), making a statement about their homology to the arachnopulmonate and solifuge DMC/DPCs difficult.

Pycnogonida lend support for a set of ancestral SIFa-lir protocerebral neurons in Chelicerata

Pycnogonida or sea spiders are the closest related group to euchelicerates (Ballesteros et al., 2022; Ballesteros & Sharma, 2019; Sharma & Gavish-Regev, 2024). Brenneis (in prep.) could show that pycnogonids have distinct stereotypic sets of SIFa-lir neurons, not only in the VNS but also in the brain. Consistent across multiple species studied, each protocerebral hemisphere displays one dorsomedial soma that projects its primary neurite anterior to the arcuate body and one anteroventral pair of somata. The primary neurites of both neuron types cross contralaterally into the other protocerebral half and descend through the deutocerebral neuropil into the VNS (Fig. 19). Although further investigations are needed to decipher the longitudinal projections in the VNS in more detail, at least some (if not even all) of them extend along its entire length and form a loop posteriorly. This strongly resembles the projections of the DMCs/DPCs in arachnopulmonates and solifuges. In addition to these consistently labelled neuron types, representatives of some pycnogonid families display additional SIFa-lir brain neurons and/or the dorsomedial and anteroventral somata exhibit additional neurite branches (Fig. 19). This is indicative of taxon-specific modifications similar to the euchelicerate taxa investigated in this study. Taken together, similarities between the dorsomedial neurons of pycnogonids with their characteristic projections and the DMCs/DPCs in euchelicerates strongly suggests their homology. Accordingly, it is here proposed that this neuron type is part of the chelicerate ground pattern.

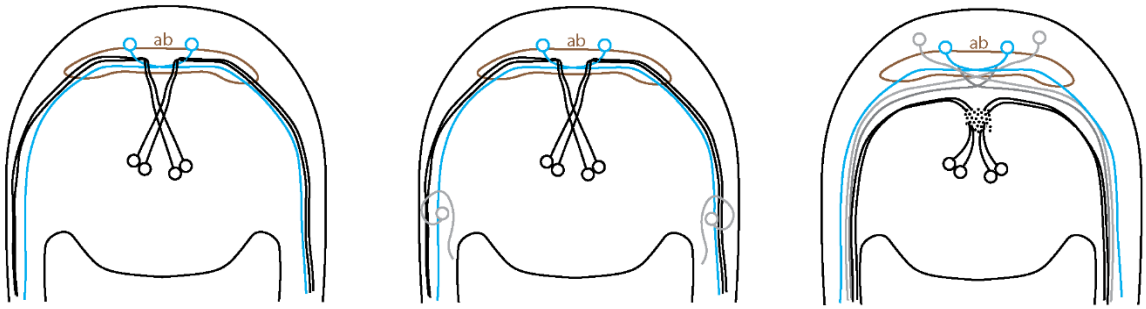

Figure 19: Schematic drawings of SIFa-lir neurons of the brain in three different pycnogonid species (from left to right: *Ammothea clausi*, *Ammothea meridionalis* and *Nymphon gracile*). Anterodorsal view. Proposed homologous neurons are shown in light blue. The deduced minimal ground pattern of neurons and their projections are depicted in black. Additional somata and/or projections are greyed out.

Abbreviations: ab = arcuate body

Comparison to SIFa-lir patterns in other arthropods

SIFamide and its expression in CNS neurons have been widely studied in several insect groups (see Arendt et al., 2015; Gellerer et al., 2014; Verleyen et al., 2004; Verleyen et al., 2009). Interestingly, they all share one pair of SIFamidergic neurons per body half with somata in the pars intercerebralis, located in the anteromedian part of the protocerebrum (Arendt et al., 2015; Gellerer et al., 2014; Verleyen et al., 2004; Verleyen et al., 2009), bearing strong resemblance to the DMCs/DPCs in the euchelicerates as well as the dorsomedial somata in the pycnogonids. As in the chelicerates, the main neurites of these cells project into the VNS after crossing contralaterally (Arendt et al., 2015; Gellerer et al., 2014; Verleyen et al., 2004; Verleyen et al., 2009). In addition to those four pars intercerebralis neurons, there are other protocerebral taxon-specific neurons found in some insect species, including cockroaches (Arendt et al., 2015) and the desert locust (Gellerer et al., 2014).

In contrast to insects, the few crustaceans studied are much more variable in the patterns of their SIFamide-immunoreactive neurons, with SIFamidergic signal being reported for all compartments of the brain (Polanska et al., 2007; Raspe et al., 2023; Yasuda-Kamatani and Yasuda, 2006; Yasuda et al., 2004). Yasuda et al. (2004; 2006) described clusters of neuronal somata whereas Polanska et al. (2007) and Raspe et al. (2023) were able to identify individual neurons. Although none of them were able to trace the neuronal projections with

confidence, similar elements such as a crossing of neurites in the brain of the marbled crayfish have been described (Polanska et al., 2007). Furthermore, two paired somata in the lateral protocerebrum of the amphipod *Parhyale hawaiensis* were proposed to be potentially homologous to the somata of the pars intercerebralis in insects (Raspe et a., 2023). Unfortunately, detailed insights into the SIFamidergic patterns in the VNS of crustacean taxa is lacking. To date, only SIFa-lir varicosities in the VNS of the *P. hawaiensis* have been described (Raspe et al., 2023) and the mere presence of SIFamide in the thoracic ganglion of the giant tiger prawn *Penaeus monodon* has been confirmed without identification of neuronal somata (Chansela et al., 2012). As a consequence, additional research is necessary to enable a more informed comparison between crustacean SIFamidergic patterns and those in other arthropod groups, including insects and chelicerates.

Conclusion and future directions

In this study, the SIFa-lir pattern in the CNS of five orders of euchelicerates has been investigated (not counting the preliminary results of the xiphosurans) and compared among each other and with other arthropod groups. Although several aspects in the SIFamide-immunoreactive neuronal patterns differ between species and more inclusive taxa, there are some elements that share notable morphological similarities across all groups that have been studied in enough detail. These similarities are most striking in the case of the DMCs/DPCs of euchelicerates, the dorsomedial neurons of pycnogonids and the neurons in in the insect pars intercerebralis. The somata of these neurons are consistently located in the protocerebrum, their primary neurites arborize through the brain neuropil, cross contralaterally, descend into the VNS and project longitudinally along its entire length. Adhering to criteria for homologization of individually identifiable neurons suggested by Kutsch and Breidbach (1994) – including size, position, trajectories and termination sites of the respective neurons – the present study therefore proposes that these SIFa-lir neurons are homologous across arthropods. In the grand scheme of arthropod evolution, this would mean that these neurons were already present in the protocerebrum of the last common

ancestor of all arthropods and thus represent a plesiomorphic feature of the chelicerate ground pattern.

It would be very interesting and also necessary to take a closer look at other representatives of the remaining orders to be capable of providing relevant information regarding SIFa-lir patterns and internal chelicerate phylogeny. The presence of the proposed homologous neuron types in nearly all euchelicerate taxa examined in this study, unfortunately cannot contribute to the current debate of the euchelicerate relationships.

Notably, this study provides strictly morphological descriptions of SIFa-lir neurons. Accordingly, no reliable conclusions about the function of SIFamide in euchelicerates can be drawn. Given the various functions of SIFamide in selected arthropod species studied, further research addressing the SIFamide function in chelicerates must be implemented to evaluate if any conserved functional role(s) can be inferred for the arthropod lineage.

Literature

Arendt, A., Neupert, S., Schendzielorz, J., Predel, R., Stengl, M. (2016). The neuropeptide SIFamide in the brain of three cockroach species. Journal of Comparative Neurology, 524(7), 1337–1360. https://doi.org/10.1002/cne.23910

Babu, K. S. (1985). Patterns of arrangement and connectivity in the central nervous system of arachnids. In: Barth, F. G. (eds) Neurobiology of arachnids. Springer, Berlin, Heidelberg. https://doi.org/10.1007/978-3-642-70348-5_1

Ballesteros, J., A., Santibáñez-López C. E., Baker, C. M., Benavides, L. R., Cunha, T. J., Gainett, G., Ontano, A. Z., Setton, E. V. W., Arango C. P., Gavish-Regev, E., Harvey, M. S., Wheeler, W. C., Hormiga, G., Giribet, G., Sharma, P. P. (2022). Comprehensive species sampling and sophisticated algorithmic approaches refute the monophyly of Arachnida. Molecular Biology and Evolution, 39. https://doi.org/10.1093/molbev/msac021

Ballesteros, J. A., Santibáñez López, C. E., Kováč, Ľ., Gavish-Regev, E., & Sharma, P. P. (2019). Ordered phylogenomic subsampling enables diagnosis of systematic errors in the placement of the enigmatic arachnid order Palpigradi. Proceedings of the Royal Society B: Biological Sciences, 286(1917), 20192426. https://doi.org/10.1098/rspb.2019.2426

Ballesteros, J. A., Setton, E. V. W., Santibáñez-López, C. E., Arango, C. P., Brenneis, G., Brix, S., Corbett, K. F., Cano-Sánchez, E., Dandouch, M., Dilly, G. F., Eleaume, M. P., Gainett, G., Gallut, C., McAtee, S., McIntyre, L., Moran, A. L., Moran, R., López-González, P. J., Scholtz, G., Williamson, C., Woods, H. A., Zehms, J. T., Wheeler, W. C., Sharma, P. P. (2021). Phylogenomic resolution of sea spider diversification through integration of multiple data classes. Molecular Biology and Evolution, 38, 686–701. https://doi.org/10.1093/molbev/msaa228

Ballesteros, J. A., Sharma P. P. (2019). A critical appraisal of the placement of Xiphosura (Chelicerata) with account of known sources of phylogenetic error. Systematic Biology, 68, 896–917. https://doi.org/10.1093/sysbio/syz011

Brusca, R., Giribet, G., Moore, W. (2023). Invertebrates, 4th ed.

Brenneis, G. (2022). The visual pathway in sea spiders (Pycnogonida) displays a simple serial layout with similarities to the median eye pathway in horseshoe crabs. BMC Biology 20, 27 https://doi.org/10.1186/s12915-021-01212-z

Brenneis, G., Scholtz, G. (2015). Serotonin-immunoreactivity in the ventral nerve cord of Pycnogonida – support for individually identifiable neurons as ancestral feature of the arthropod nervous system. BMC Evolutionary Biology, 15(136). https://doi.org/10.1186/s12862-015-0422-1

Chansela, P., Goto-Inoue, N., Zaima, N., Sroyraya, M., Sobhon, P., & Setou, M. (2012). Visualization of neuropeptides in paraffin-embedded tissue sections of the central nervous system in the decapod crustacean, *Penaeus monodon*, by imaging mass spectrometry. Peptides, 34(1), 10–18. https://doi.org/10.1016/j.peptides.2011.03.021

Christie, A. E., Chi, M. (2015). Neuropeptide discovery in the Araneae (Arthropoda, Chelicerata, Arachnida): Elucidation of true spider peptidomes using that of the western black widow as a reference. General and Comparative Endocrinology, 213, 90-109. https://doi.org/10.1016/j.ygcen.2015.02.003

Christie, A. E., Nolan, D. H., Ohno, P., Hartline, N., Lenz, P. H. (2011). Identification of chelicerate neuropeptides using bioinformatics of publicly accessible expressed sequence tags. General and Comparative Endocrinology, 170, 144-155. https://doi.org/10.1016/j.ygcen.2010.09.018

Doeffinger, C., Hartenstein, V., Stollewerk, A. (2010). Compartmentalization of the precheliceral neuroectoderm in the spider *Cupiennius salei*: Development of the arcuate body, optic ganglia, and mushroom body. Journal of Comparative Neurology, 518(13), 2612–2632. https://doi.org/10.1002/cne.22355

Drozd, D., Wolf, H., Stemme, T. (2020). Structure of the pecten neuropil pathway and its innervation by bimodal peg afferents in two scorpion species. PLOS ONE 15(12): e0243753. https://doi.org/10.1371/journal.pone.0243753

Fabian-Fine, R., Volknandt, W., Seyfarth, E. A. (1999). Peripheral synapses at identifiable mechanosensory neurons in the spider *Cupiennius salei* : synapsin-like immunoreactivity. Cell and Tissue Research 295, 13–19. https://doi.org/10.1007/s004410051208

Firstman, B. (1973). The relationship of the chelicerate arterial system to the evolution of the endosternite. The Journal of Arachnology, 1(1), 1–54. http://www.jstor.org/stable/3705296

Frankowski, K., Miyazaki, K., Brenneis, G. (2022). A microCT-based atlas of the central nervous system and midgut in sea spiders (Pycnogonida) sheds first light on evolutionary trends at the family level. Frontiers in Zoology 19, 14. https://doi.org/10.1186/s12983-022-00459-8

Gainett, G., Klementz, B. C., Setton, E. V. W., Simian, C., Iuri, H. A., Edgecombe, G. D., Peretti, A. V., Sharma, P. P. (2024). A plurality of morphological characters need not equate with phylogenetic accuracy: A rare genomic change refutes the placement of Solifugae and Pseudoscorpiones in Haplocnemata. Evolution & Development, 26, e12467. https://doi.org/10.1111/ede.12467

Garwood, R. J., Dunlop, J. A. (2023). Consensus and conflict in studies of chelicerate fossils and phylogeny. Arachnologische Mitteilungen: Arachnology Letters, 66(1), 2–16. https://doi.org/10.30963/aramit6602

Gellerer A., Franke, A., Neupert, S., Predel, R., Zhou, X., Liu, S., Reiher, W., Wegener, C., Homberg, U. (2015). Identification and distribution of SIFamide in the nervous system of the desert locust Schistocerca gregaria. Journal of Comparative Neurology, 523, 108-125. https://doi.org/10.1002/cne.23671

Hanström B. (1928). Das Nervensystem der wirbellosen Tiere. Springer, Berlin, Heidelberg, New York.

Harzsch, S. (2004). Phylogenetic comparison of serotonin-immunoreactive neurons in representatives of the Chilopoda, Diplopoda, and Chelicerata: Implications for arthropod relationships. Journal of Morphology, 259, 198-213. https://doi.org/10.1002/jmor.10178

Harzsch, S., Müller, C.H.G., Wolf, H. (2005). From variable to constant cell numbers: cellular characteristics of the arthropod nervous system argue against a sister-group relationship of Chelicerata and “Myriapoda” but favour the Mandibulata concept. Development Genes and Evolution, 215, 53–68. https://doi.org/10.1007/s00427-004-0451-z

Harzsch, S., Waloszek, D. (2000). Serotonin-immunoreactive neurons in the ventral nerve cord of Crustacea: a character to study aspects of arthropod phylogeny. Arthropod Structure & Development, 29, 307-322. https://doi.org/10.1016/S1467-8039(01)00015-9

Howard, R. J., Puttick, M. N., Edgecombe G. D., Lozano-Fernandez, J. (2020). Arachnid monophyly: Morphological, palaeontological and molecular support for a single terrestrialization within Chelicerata. Arthropod Structure & Development, 59, 100997. https://doi.org/10.1016/j.asd.2020.100997

Kutsch, W., Breidbach, O. (1994). Homologous structures in the nervous systems of Arthropoda, Editor(s): P.D. Evans, Advances in Insect Physiology, Academic Press, 24, 1-113. https://doi.org/10.1016/S0065-2806(08)60082-X

Loesel, R., Wolf, H., Kenning, M., Harzsch, S., Sombke, A. (2013). Architectural principles and evolution of the arthropod central nervous system. In: Minelli, A., Boxshall, G., Fusco, G. (eds) Arthropod Biology and Evolution. Springer, Berlin, Heidelberg. https://doi.org/10.1007/978-3-642-36160-9_13

Lozano-Fernandez, J., Tanner, A. R., Giacomelli, M., Carton, R., Vinther, J., Edgecombe, G. D., Pisani, D. (2019). Increasing species sampling in chelicerate genomic-scale datasets provides support for monophyly of Acari and Arachnida. Nature Communications, 10(1), 2295. https://doi.org/10.1038/s41467-019-10244-7

Maurer, M., Hladik, J., Iliffe, T. M., Stemme, T. (2019). Histaminergic interneurons in the ventral nerve cord: assessment of their value for Euarthropod phylogeny. Zoological Letters 5, 36. https://doi.org/10.1186/s40851-019-0151-1

Munilla, T., Nieto, D. (1999). Littoral pycnogonids from the Chafarinas Islands (Alboran Sea, Western Mediterranean). Vie et Milieu / Life & Environment, 155-161.

Nolan, E. D., Santibáñez-López, C. E., Sharma, P. P. (2020). Developmental gene expression as a phylogenetic data class: Support for the monophyly of Arachnopulmonata. Development Genes and Evolution, 230(2), 137–153. https://doi.org/10.1007/s00427-019-00644-6

Ontano, A. Z., Gainett, G., Aharon, S., Ballesteros, J. A., Benavides, L. R., Corbett, K. F., Gavish-Regev, E., Harvey, M. S., Monsma, S., Santibáñez-López, C. E., Setton, E. V. W., Zehms, J. T., Zeh, J. A., Zeh, D. W., Sharma, P. P. (2021). Taxonomic sampling and rare genomic changes overcome long-branch attraction in the phylogenetic placement of pseudoscorpions. Molecular Biology and Evolution, 38, 2446–2467. https://doi.org/10.1093/molbev/msab038

Polanska, M. A., Yasuda, A., Harzsch, S. (2007). Immunolocalisation of crustacean-SIFamide in the median brain and eyestalk neuropils of the marbled crayfish. Cell and Tissue Research, 330, 331–344. https://doi.org/10.1007/s00441-007-0473-8

Raspe, S., Kümmerlen, K., Harzsch, S. (2023). Immunolocalization of SIFamide-like neuropeptides in the adult and developing central nervous system of the amphipod *Parhyale hawaiensis* (Malacostraca, Peracarida, Amphipoda). Arthropod Structure & Development, 77, 101309. https://doi.org/10.1016/j.asd.2023.101309

Regier, J. C., Shultz, J. W., Zwick, A., Hussey, A., Ball, B., Wetzer, R., Martin, J. W., & Cunningham, C. W. (2010). Arthropod relationships revealed by phylogenomic analysis of nuclear protein-coding sequences. Nature, 463(7284), 1079–1083. https://doi.org/10.1038/nature08742

Richter, S., Loesel, R., Purschke, G., Schmidt-Rhaesa, A., Scholtz, G., Stach, T., Vogt, L., Wanninger, A., Brenneis, G., Döring, C., Faller, S., Fritsch, M., Grobe, P., Heuer, C. M., Kaul, S., Møller, O. S., Müller, C. H., Rieger, V., Rothe, B. H., Stegner, M. E., Harzsch, S. (2010). Invertebrate neurophylogeny: Suggested terms and definitions for a neuroanatomical glossary. Frontiers in Zoology, *7*(1), 29. https://doi.org/10.1186/1742-9994-7-29

Riehle, M. A., Garczynski, S. F., Crim, J. W., Hill, C. A., Brown, M. R. (2002). Neuropeptides and peptide hormones in *Anopheles gambiae*. Science 298, 172–175. https://doi.org/10.1126/science.1076827

Sharma, P. P., Gavish-Regev, E. (2024). The evolutionary biology of Chelicerata. Annual Review of Entomology, 70, 143–63. https://doi.org/10.1146/annurev-ento-022024-011250

Sharma, P. P., Schwager, E. E., Extavour, C. G., Wheeler, W. C. (2014). Hox gene duplications correlate with posterior heteronomy in scorpions. Proceedings of the Royal Society B: Biological Sciences, 281(1792), 20140661. https://doi.org/10.1098/rspb.2014.0661

Shultz, J. W. (2007). A phylogenetic analysis of the arachnid orders based on morphological characters. Zoological Journal of the Linnean Society, 150(2), 221–265. https://doi.org/10.1111/j.1096-3642.2007.00284.x

Šimo, L., Itňan, D. Ž., Park, Y. (2009). Two novel neuropeptides in innervation of the salivary glands of the black-legged tick, *Ixodes scapularis*: Myoinhibitory peptide and SIFamide. Journal of Comparative Neurology, 517(5), 551–563. https://doi.org/10.1002/cne.22182

Šimo, L., Koči, J., Kim, D., Park, Y. (2014), Invertebrate specific D1-like dopamine receptor in control of salivary glands in the black-legged tick *Ixodes scapularis*. Journal of Comparative Neurology, 522, 2038-2052. https://doi.org/10.1002/cne.23515

Sinakevitch, I., Long, S. M., Gronenberg, W. (2021). The central nervous system of whip spiders (Amblypygi): Large mushroom bodies receive olfactory and visual input. Journal of Comparative Neurology, 529, 1642-1658. https://doi.org/10.1002/cne.25045

Smarandache-Wellmann, C. R. (2016). Arthropod neurons and nervous system. Current Biology, 26(20), R960–R965. https://doi.org/10.1016/j.cub.2016.07.063

Sombke, A., Stemme, T. (2017). Serotonergic neurons in the ventral nerve cord of Chilopoda – a mandibulate pattern of individually identifiable neurons. Zoological Letters, 3(9). https://doi.org/10.1186/s40851-017-0070-y

Steinhoff, P. O. M., Harzsch, S., Uhl, G. (2024). Comparative neuroanatomy of the central nervous system in web-building and cursorial hunting spiders. Journal of Comparative Neurology, 532(2), e25554. https://doi.org/10.1002/cne.25554

Steinhoff, P. O. M., Sombke, A., Liedtke, J., Schneider, J. M., Harzsch, S., Uhl, G. (2017). The synganglion of the jumping spider *Marpissa muscosa* (Arachnida: Salticidae): Insights from histology, immunohisto-chemistry and microCT analysis. Arthropod Structure and Development, 46(2), 156–170. https://doi.org/10.1016/j.asd.2016.11.003

Steinhoff, P. O. M., Uhl, G., Harzsch, S., Sombke, A. (2020). Visual pathways in the brain of the jumping spider *Marpissa muscosa*. The Journal of Comparative Neurology, 528(11), 1883–1902. https://doi.org/10.1002/cne.24861

Stemme, T., Pfeffer, S. E. (2022). Anatomy of the nervous system in *Chelifer cancroides* (Arachnida: Pseudoscorpiones) with a distinct sensory pathway associated with the pedipalps. Insects, 3(25). https://doi.org/10.3390/insects13010025

Stemme, T., Stern, M., Bicker, G. (2017). Serotonin-containing neurons in basal insects: In search of ground patterns among Tetraconata. Journal of Comparative Neurology, 525, 79-115. https://doi.org/10.1002/cne.24043

Stock, J. H. (1994). Indo-West Pacific Pycnogonida collected by some major oceanographic expeditions. Beaufortia, Institute for Systematics and Population Biology University of Amsterdam, 44(3).

Ungerer, P., Scholtz, G. (2008). Filling the gap between identified neuroblasts and neurons in crustaceans adds new support for Tetraconata. Proceedings of the Royal Society B: Biological Sciences, 275, 369–376. http://doi.org/10.1098/rspb.2007.1391

Verleyen, P., Huybrechts, J., Baggerman, G., Van Lommel, A., De Loof, A., Schoofs, L. (2004). SIFamide is a highly conserved neuropeptide: A comparative study in different insect species. Biochemical and Biophysical Research Communications, 320(2), 334–341. https://doi.org/10.1016/j.bbrc.2004.05.173

Verleyen, P., Huybrechts, J., Schoofs, L. (2009). SIFamide illustrates the rapid evolution in arthropod neuropeptide research. General and Comparative Endocrinology, 162(1), 27-35. https://doi.org/10.1016/j.ygcen.2008.10.020

Wolf, H., Harzsch, S. (2012). Serotonin-immunoreactive neurons in scorpion pectine neuropils: similarities to insect and crustacean primary olfactory centres?. Zoology, 115, 151-159. https://doi.org/10.1016/j.zool.2011.10.002

Yasuda, A., Yasuda-Kamatani, Y., Nozaki, M., Nakajima, T. (2004). Identification of GYRKPPFNGSIFamide (crustacean-SIFamide) in the crayfish *Procambarus clarkii* by topological mass spectrometry analysis. General and Comparative Endocrinology, 135(3), 391–400. https://doi.org/10.1016/j.ygcen.2003.10.001

Yasuda-Kamatani, Y., Yasuda, A. (2006). Characteristic expression patterns of allatostatin-like peptide, FMRFamide-related peptide, orcokinin, tachykinin-related peptide, and SIFamide in the olfactory system of

crayfish *Procambarus clarkii*. Journal of Comparative Neurology, 496(1), 135–147. https://doi.org/10.1002/cne.20903